

AN ANALYTIC STUDY OF THE BAROCLINIC INSTABILITY PROBLEM
ON THE SPHERE

by

YUNG-AN LEE

B.S., Atmospheric Science, National Taiwan University
(1979)

SUBMITTED TO THE DEPARTMENT OF
EARTH, ATMOSPHERIC, AND PLANETARY SCIENCES
IN PARTIAL FULFILLMENT OF THE
REQUIREMENTS FOR THE DEGREE OF

DOCTOR OF PHILOSOPHY

at the

MASSACHUSETTS INSTITUTE OF TECHNOLOGY
September, 1987

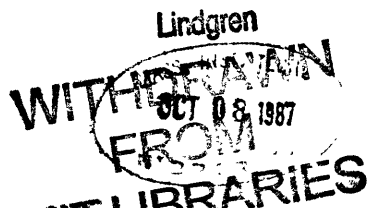
© Yung-An Lee, 1987

The author hereby grants to M.I.T. permission to reproduce and to
distribute copies of this thesis document in whole or in part

Signature of Author.....
Department of Earth, Atmospheric, and Planetary Sciences
September, 1987

Certified by.....
Professor Peter H. Stone
Thesis Supervisor

Accepted by.....
Chairman, Departmental Committee on Graduate Students



**AN ANALYTIC STUDY OF THE BAROCLINIC INSTABILITY
PROBLEM ON THE SPHERE**

by

YUNG-AN LEE

Submitted to the Department of Earth, Atmospheric, and Planetary Sciences on September 4, 1987 in partial fulfillment of the requirements for the degree of Doctor of Philosophy.

ABSTRACT

An analytical study of baroclinic instability on the sphere is presented. We study analogues of both Eady's and Charney's problems on the sphere. Furthermore, we derive analytic solutions for the problem of a general meridional profile of the basic flow.

The governing equation is the quasigeostrophic potential vorticity equation on the sphere. We adopt a shortwave approximation and a two-scale assumption to derive the approximate solutions for these problems. These solutions contain a second-order turning point whose location is very important in determining the properties of the unstable waves. This second-order turning point is located at the maximum of the meridional temperature gradient and, because of the variation of the Coriolis parameter, it is always located on the poleward side of the westerly zonal flow maximum.

Furthermore, the analytic solutions indicate a very close relation between baroclinic instability on the sphere and that on a β -plane. In fact, if β -plane is located at the latitude of the turning point, the study of a uniform zonal flow should be able to correctly derive most of the properties of the baroclinic unstable waves on the sphere. Nonetheless, the spherical geometry and the meridional profile of the basic flow have significant effects on the perturbation's meridional structure and the eddy momentum flux, which can not be correctly predicted by a β -plane study.

Although the analytic solutions have some limitations and are not valid for long waves, they are still able to capture the essential features of baroclinic instability on the sphere. Furthermore, these have implications for parameterizations of the eddy fluxes in climate modeling and allow one to predict the properties of the unstable waves for given meridional profiles of the basic flow, which may be useful for guiding numerical studies.

Thesis Supervisor: Peter H. Stone
Title: Professor of Meteorology

DEDICATION

To

My father and mother

ACKNOWLEDGEMENTS

I thank my advisor, Professor Peter Stone, for his insights that motivated this thesis. I have benefited greatly from his helpful guidance and suggestions. I also benefited from discussions with Professors Edward Lorenz, Glenn Flierl and Kerry Emanuel. I want to thank Jane McNabb in Center headquarters and many people in and about Cambridge to whom I am eternally grateful for their advice, support, and friendship during my stay at MIT. As a foreign student, I am grateful for the opportunity to pursue an advanced degree at MIT. During these years, I was supported through National Aeronautics and Space Administration grant NASA/G-g NSG 5113.

TABLE OF CONTENTS

	Page
Abstract.....	2
Dedication.....	4
Acknowledgements.....	5
Table of Contents.....	6
List of Figures.....	7
I. Introduction.....	10
II. The Governing Equation.....	21
III. An Analogue of Eady's Model on the Sphere.....	35
IV. An Analogue of Charney's Model on the Sphere.....	50
V. A General Meridional Profile Problem.....	90
VI. Summary and Conclusion.....	127
References.....	131
Biographical Note.....	134

LIST OF FIGURES

	Page
Fig. 1.1. The phase speeds(upper) and growth rates(lower) as functions of the total wavenumber from the exact results(short dashes) of Lindzen and Rosenthal(1981) and the shortwave approximation(solid), taken from Branscome(1983).....	17
Fig. 2.1. The growth rates(a) and phase speeds(b) from Lorenz's model(solid) and approximated equation(dashes) as function of zonal wavenumber, taken from fig.1 of Hollingsworth, Simmons and Hoskins(1976).....	27
Fig. 2.2. The perturbation's phases(a) and amplitudes(b) as functions of latitude from both Lorenz's model(upper) and approximated equation(lower), taken from fig. 2 and fig. 3 of Hollingsworth, Simmons and Hoskins(1976).....	28
Fig. 3.1. The meridional structure of the basic flow as a function of latitude at $z=1$	45
Fig. 3.2. The growth rate as a function of zonal wave number for each meridional wave number n , $n=1,2,3$	48
Fig. 3.3. As in fig. 2.2, except for the steering level.....	48
Fig. 3.4. The amplitude and phase of the most unstable wave, $k=6$ and $n=1$, as a function of height.....	49
Fig. 3.5. The amplitude of the most unstable wave as a function of latitude....	49
Fig. 4.1. The perturbation's growth rates for solid body rotation as functions of the zonal wavenumber k for $U_0 = 20, 30$ and 40 m/sec. $N_0^2 = 2 \times 10^{-4} \text{ sec.}^{-2}$ and other basic state parameters the same as chapter iii.....	77
Fig. 4.2. As in Fig. 4.1, except for the phase speeds.....	77
Fig. 4.3. As in Fig. 4.1, except for the cases of $N_0^2 = 1 \times 10^{-4}, 2 \times 10^{-4}, 3 \times 10^{-4} \text{ sec.}^{-2}$. The value of U_0 is taken as $U_0 = 30 \text{ m sec}^{-1}$	78

Fig. 4.4.	As in Fig. 4.3, except for the phase speeds.....	78
Fig. 4.5.	The location of the perturbation's maximum amplitude as a function of the zonal wavenumber k for $U_0=20, 30$ and 40 m/sec..	81
Fig. 4.6.	As in Fig. 4.5, except for: $N_0^2 = 1 \times 10^{-4}, 2 \times 10^{-4}, 3 \times 10^{-4}$ sec ⁻²	81
Fig. 4.7.	The meridional amplitude functions of $k= 8, 16, 24$ and $n=1$ for $U_0=30$ m/sec. and $N_0^2= 2 \times 10^{-4}$ sec. ⁻²	82
Fig. 4.8.	As in Fig. 4.7, except for the meridional phase variation.....	82
Fig. 4.9.	As in Fig. 4.7, except for the amplitudes as functions of height at the turning point, which is located at 45^0 latitude.....	84
Fig. 4.10.	As in Fig. 4.7, except for the vertical phase variations.....	84
Fig. 4.11.	As in Fig. 4.7, except for the eddy momentum fluxes.....	85
Fig. 4.12.	As in Fig. 4.9, except for the eddy heat fluxes at the turning point..	85
Fig. 5.1.	The meridional cross sections of the basic flows and temperatures for the 30^0 jet (a), the 55^0 jet (b), and for solid body rotation (c), taken from Simmons and Hoskins(1976).....	104
Fig. 5.2.	The perturbation's growth rates as functions of the zonal wavenumber for the solid body rotation: the "Short wave" results were calculated from (5.58), the PE and QG results, taken from Simmons and Hoskins(1976), were calculated from the primitive equations and the quasigeostrophic equations, respectively.....	108
Fig. 5.3.	As in fig. 5.2, except for the phase speeds.....	108
Fig. 5.4.	The perturbation's growth rates as functions of the zonal wavenumber for the 30^0 jet.....	109
Fig. 5.5.	As in fig. 5.4, except for the phase speeds.....	109
Fig. 5.6.	The perturbation's growth rates as functions of the zonal wavenumber for the 55^0 jet.....	110
Fig. 5.7.	As in fig. 5.4, except for the phase speeds.....	110

- Fig. 5.8. The locations of the perturbation's maximum amplitude as functions of the zonal wavenumber for the solid body rotation, the 30^0 jet and for the 55^0 jet. The straight lines are the locations of the turning points for these three profiles.....113
- Fig. 5.9. The meridional amplitude and phase of the zonal wavenumber 8 as functions of latitude for the solid body rotation.....113
- Fig. 5.10. As in fig.5.9, except for the 30^0 jet.....114
- Fig. 5.11. As in fig.5.9, except for the 55^0 jet.....114
- Fig. 5.12. The perturbation's steering levels at the turning point as functions of the zonal wavenumber for the solid body rotation, the 30^0 jet and for the 55^0 jet.....117
- Fig. 5.13. The amplitudes of the zonal wavenumber 8 at the turning points as functions of height for the solid body rotation, the 30^0 jet and for the 55^0 jet.....117
- Fig 5.14. As in fig. 5.13, except for the leading order phase of the vertical structure.....118
- Fig. 5.15. As in fig. 5.13, except for the eddy heat fluxes.....123
- Fig. 5.16. The eddy momentum fluxes of zonal wavenumber 8 as functions of latitude for the solid body rotation, the 30^0 jet and for the 55^0 jet...123
- Fig. 5.17. The meridional cross sections of the eddy momentum fluxes at wavenumber 8 for the 30^0 jet (a), the 55^0 jet (b) and for solid body rotation (c), taken from Simmons and Hoskins(1976).....124

CHAPTER I

INTRODUCTION

Since the pioneering works of Charney(1947) and Eady(1949), the theoretical study of baroclinic instability has been one of the most important topics in atmospheric dynamics. In the literature, there are two different geometrical assumptions in the studies of baroclinic instability; one is plane geometry and the other is spherical geometry. The difference in geometry has led to somewhat different approaches to studying the problem. Both analytic and numerical analyses have been adopted to investigate the baroclinic instability problem in plane geometry, but only numerical analyses have been used to study this problem on the sphere. Furthermore, although many aspects of baroclinic instability are similar in both geometries, there are some aspects that remain to be understood.

The purposes of this study are: (1). to find an analytic solution for the baroclinic instability problem on the sphere; (2). to learn how the properties of the baroclinic unstable waves on the sphere are determined; (3). to find out the effects of the spherical geometry and the meridional profile of the basic flow on the behavior of these unstable waves.

In the following, we shall discuss the effects of these two geometrical assumptions on the methods applied to study the

baroclinic instability problem. Also, we shall discuss the similarities and differences between the results with these different geometries.

(a). the plane geometry

Since the work of Charney(1947), the plane geometry assumption has been adopted in most of the theoretical studies of baroclinic instability. This assumption neglects the curvature effect of the earth and the meridional variation of the Coriolis parameter, except that a β -plane is used where the gradient of the Coriolis parameter is retained. With the quasigeostrophic approximation, the governing equations of the large scale atmospheric motions can be reduced to a single equation, which is the β -plane quasigeostrophic potential vorticity equation. This single governing equation not only simplifies the baroclinic instability problem in plane geometry, but also provides information about the necessary condition for instability(Charney and Stern, 1962; Pedlosky, 1964a) and bounds on the phase speed and growth rate of the perturbations. Although the plane geometry assumption is unrealistic for the earth's atmosphere, since the baroclinic instability process is mainly a midlatitude phenomenon, it can still be justified.

For a uniform zonal mean flow, the governing equation of the baroclinic instability problem is a trivial two-dimensional differential equation, which can be easily reduced to an ordinary differential equation for the perturbation's vertical structure. It is easy to solve either analytically or numerically. There are two different models

that were adopted by most of the theoretical studies in plane geometry; one is Eady's model on a f -plane and the other is Charney's model on a β -plane.

(i). Eady's Model

Eady(1949) introduced the simplest model on a f -plane, where the β -effect is neglected, that displays the baroclinic instability process. The basic state of this model has constant density and static stability. The mean flow is a linear function of height without meridional variation. Since there is no basic state potential vorticity gradient in the governing equation, the necessary condition of instability can be satisfied if both upper and lower boundaries be horizontal rigid planes. Since the basic state potential vorticity gradient is zero, the equation and the boundary conditions are very simple. Therefore this instability problem can be solved analytically without any difficulty.

The results of this problem show that the instability only occurs at low zonal wavenumbers. Since, as the wave becomes shorter, the perturbation will be trapped near one of the boundaries, the necessary condition for instability can no longer be satisfied. Therefore, there is a shortwave cutoff for instability. The lowest meridional wavenumber has the largest growth rate. The most unstable wave has a zonal scale similar to the synoptic scale eddies of the atmosphere. The phase speeds are the same for all unstable waves. The unstable waves have the same vertical scale as that of

the mean flow. The amplitudes of the unstable waves have a minimum near mid-level and increase toward both boundaries. The phase of these unstable waves tilts westward and upward, which is the same condition for the baroclinic conversion of energy from the mean field to the perturbation. Furthermore the eddy heat flux is poleward everywhere. Since the basic flow has no meridional variation, there is no eddy momentum flux in this model.

(ii). Charney's Model

Charney(1947) studied a more realistic model that retains both the β term and the vertical variation of the basic state density, which is an exponentially decreasing function of height. The basic state potential vorticity gradient is no longer zero in this model. Therefore, from the necessary condition for instability, the upper rigid boundary condition can be relaxed and replaced by the radiation condition at infinity.

From the discussion of Held(1978), Branscome(1983) and Pedlosky(1987), the existence of a nonzero basic state potential vorticity gradient has two significant effects on this baroclinic instability problem. One is that there is a singularity in the governing equation and the other is that there are important changes in the vertical and horizontal scales of the unstable disturbances.

Due to the presence of a singularity in the governing equation, it is more difficult to find an analytic solution for this baroclinic

instability problem. Though analytic solutions did not exist in the original work of Charney, they were derived in later studies(Kuo, 1952, 1973; Lindzen and Rosenthal, 1981 and etc.). Nonetheless, these solutions were very complex. It required numerical calculations to determine the perturbation's growth rate, phase speed and other properties.

Branscome(1983) introduced a shortwave approximation to simplify this baroclinic instability problem. The shortwave approximation assumes that the perturbation's total wavenumber is larger than other terms in the governing equation. Therefore, after rescaling, the basic state potential vorticity gradient is an order smaller than other terms in the resulting equation. Then he applied a perturbation method to solve the equation. Since the basic state potential vorticity gradient is not present in the leading order equation, the perturbation solutions are much easier to find. Moreover these perturbation solutions are much simpler than the exact solutions. Therefore the properties of the unstable baroclinic waves are more explicit and can be determined without complicated numerical calculations.

Fig. 1.1, taken from Branscome(1983), shows the phase speeds and growth rates as functions of the total wavenumber, which is scaled by the radius of deformation, from the results of both Lindzen and Rosenthal(1981) and this shortwave approximation. We note that, although these perturbation solutions from the shortwave

approximation are not valid for the whole wave spectrum, they do give reasonable results even at synoptic scale wavenumbers.

Furthermore, we see that only certain neutral points exist in the solutions. There is no shortwave cutoff for instability. This is due to the existence of a nonzero basic state potential vorticity gradient, i.e., as the wave becomes shorter, the vertical scale also shrinks proportionally so that the instability can still occur. Therefore, in contrast with Eady's model, the presence of the basic state potential vorticity gradient allows the unstable perturbations in Charney's model to select their own vertical scale.

The phase speeds of the unstable waves are near the minimum speed of the basic flow rather than the mean speed as in Eady's model. The maximum amplitude of the most unstable wave is at the ground. The perturbation's phase variation with height is confined near the surface, so the eddy heat flux is also confined in this region. Since there is no meridional variation in the basic flow, there is no eddy momentum flux.

For a nonuniform zonal flow, the baroclinic instability problem on a plane geometry becomes even more difficult to deal with. Since the basic flow is a function of both vertical and meridional variables, the separation of variables can not be directly applied to the governing equation. To simplify the problem, a two-scale formalism can be applied to the meridional variable to quasi-separate the equation into a vertical structure equation and a fast variation

meridional equation(Stone, 1969; Gent, 1974; Killworth, 1980; Ioannou and Lindzen, 1986). The perturbation's vertical structure equation is similar to that in the uniform zonal flow problem. The fast variation meridional structure equation is approximated by a WKB equation. Depending on the meridional domain, this equation is either a simple WKB problem(finite domain) or a two-turning-point problem(infinite domain). Then these two equations can be solved separately to determine the properties of the unstable waves.

The results from these studies showed that, in the presence of horizontal shear in the basic flow, the unstable perturbations would select their own meridional scales. Moreover, there is an eddy momentum flux associated with the unstable baroclinic waves. Pedlosky(1964b) and Stone(1969) found that this momentum flux is always against the meridional gradient of the basic flow and changes sign at the jet center.

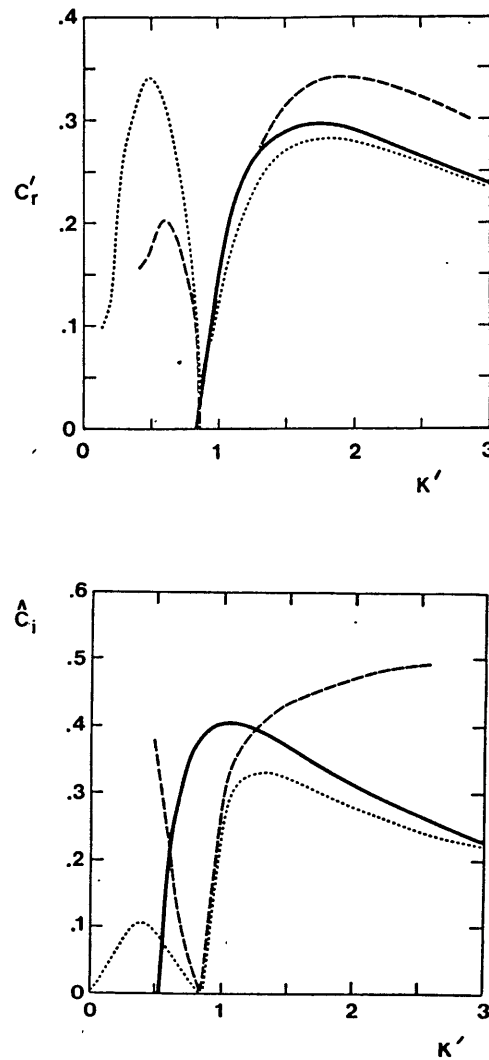


Fig. 1.1. The phase speeds (upper) and growth rates (lower) as functions of the total wavenumber from the exact results (short dashes) of Lindzen and Rosenthal(1981) and the shortwave approximation (solid), taken from Branscome(1983).

(b). the spherical geometry

On the sphere, both the earth's curvature and the full meridional variation of the Coriolis parameter are retained. The governing equations of the large scale atmospheric motions can not be easily reduced to a single equation. Although Hollingsworth, Simmons and Hoskins(1976) did introduce a quasigeostrophic potential vorticity equation on the sphere, since its coefficients depend on both meridional and vertical variables, it is more difficult to solve analytically than that in the plane geometry. Therefore, as yet, there is no analytic study of the baroclinic instability problem on the sphere.

The numerical studies(Hollingsworth, 1975; Moura and Stone, 1976; Simmons and Hoskins, 1976) showed that the eddy momentum flux is an essential feature of baroclinic instability on the sphere. They found that the stability properties and the structure of the most unstable waves are qualitatively similar to those on a β -plane, but that the spherical geometry has significant effects on the location of the disturbances and on the eddy momentum fluxes, which vary greatly from profile to profile of the basic flow.

Even though the quasigeostrophic approximation formally breaks down near equator, the quasigeostrophic equations have been used in the numerical studies of baroclinic instability on the sphere. Moura and Stone(1976) found that, since the amplitudes of unstable waves are small near the equator, the unstable solutions of the

quasigeostrophic model do not differ much from those of the balance equations. Moreover, Simmons and Hoskins(1976) showed that the results from the quasigeostrophic equations are generally similar to those of the primitive equations. Therefore, the quasigeostrophic approximation does not appear to affect the properties of baroclinic instability on the sphere.

Although a numerical analysis can investigate more realistic atmospheric flows and provide more accurate results for the baroclinic instability problem on the sphere, the determination of cause and effect relationships may be difficult. The existence of the quasigeostrophic potential vorticity equation on the sphere and the introduction of the shortwave approximation by Branscome(1983) gives us an opportunity to analytically study the baroclinic instability problem on the sphere. With this study we hope to be able to provide a link between the β -plane analytic analyses and the numerical analyses on the sphere. Also, the analytic solutions may be able to provide us information about how the perturbation's growth rate, phase speed, vertical structure, meridional structure, heat and momentum fluxes are determined. These results may be useful in improving parameterizations of the eddy fluxes in climate modeling. Moreover, we may be able to predict the structure of the perturbations for a given meridional profile of the basic flow from these analytic expressions.

In chapter ii, we present the derivation of the quasigeostrophic potential vorticity equation on the sphere and discuss the properties

of this equation. In chapter iii, we investigate an analogue of Eady's problem. In chapter iv, we study an analogue of Charney's problem and determine a proper procedure to solve the baroclinic instability problem on the sphere. In chapter v, we study the instability problem for a general meridional profile of the basic flow. In chapter vi, we summarize and conclude our study.

CHAPTER II

THE GOVERNING EQUATION

The governing equation in this study is the quasigeostrophic potential vorticity equation on the sphere, which was introduced by Hollingsworth, Simmons and Hoskins(1976). This equation, except for having coefficients which are explicit functions of latitude, is very similar to the quasigeostrophic potential vorticity equation on a β -plane. As mentioned in chapter i, the quasigeostrophic approximation did not have significant effects on the baroclinic instability problem on the sphere, so we adopt this equation as the governing equation in this study. Since there are many analytic studies(Eady, 1949; Kuo, 1952, 1973; Branscome,1983 and etc.) on a β -plane or f-plane, this similarity between the equation on the sphere and that on a β -plane may give us an important clue on how to find an analytical solution on the sphere. In this chapter, we follow the work of Hollingsworth, Simmons and Hoskins(1976) to derive the governing equation and discuss some of its properties.

This governing equation is derived from Lorenz's Model(1960), which conserves the sum of kinetic energy and available potential energy but does not allow the variation of static stability. Since the equations of Lorenz's model are in vector invariant form, they can be presented in spherical coordinates. We introduce Ψ as the streamfunction, X the velocity potential, Φ the geopotential and p the pressure. Then the equations of Lorenz's model can be written as

$$\frac{\partial}{\partial t} \nabla^2 \Psi = -J(\Psi, \nabla^2 \Psi + f) - \nabla \cdot f \nabla X \quad (2.1)$$

$$\frac{\partial T}{\partial t} = -J(\Psi, T) + \sigma \omega \quad (2.2)$$

$$\nabla^2 \Phi = \nabla \cdot f \nabla \Psi \quad (2.3)$$

$$\frac{\partial \Phi}{\partial p} = -\frac{RT}{p} \quad (2.4)$$

$$\nabla^2 X = -\frac{\partial \omega}{\partial p} \quad (2.5)$$

where

$$\sigma = -\left(\frac{\partial T_s}{\partial p} - \frac{RT_s}{c_p p} \right) \quad \text{and} \quad f = 2\Omega \mu.$$

Here T_s is the horizontal averaged temperature, $\mu = \sin(\text{latitude})$, R the gas constant, C_p the specific heat at constant pressure, Ω the angular velocity of the sphere and $\omega = dp/dt$, the vertical velocity in pressure coordinates. As noted by Hollingsworth et al., this model is essentially an energetically consistent extension to the sphere of the usual β -plane quasigeostrophic model. On the sphere,

$$J(A, B) = \frac{1}{a^2} \left(\frac{\partial A}{\partial \lambda} \frac{\partial B}{\partial \mu} - \frac{\partial A}{\partial \mu} \frac{\partial B}{\partial \lambda} \right) \quad (2.6)$$

$$\nabla A = \frac{\mathbf{i}}{a(1-\mu^2)^{1/2}} \frac{\partial A}{\partial \lambda} + \frac{\mathbf{j}}{a(1-\mu^2)^{1/2}} \frac{\partial A}{\partial \mu} \quad (2.7)$$

$$\nabla^2 A = \frac{1}{a^2} \left\{ \frac{1}{1-\mu^2} \frac{\partial^2 A}{\partial \lambda^2} + \frac{\partial}{\partial \mu} \left[(1-\mu^2) \frac{\partial A}{\partial \mu} \right] \right\} \quad (2.8)$$

where a is the radius of the sphere, λ the longitude, bold face characters, \mathbf{i} and \mathbf{j} , the unit vectors in longitudinal and latitudinal directions. By definition, the nondivergent part of wind is a function of the streamfunction; therefore the zonal and meridional parts of it can be written as

$$u = - \frac{(1-\mu^2)^{1/2}}{a} \frac{\partial \Psi}{\partial \mu} \quad (2.9)$$

$$v = \frac{1}{a(1-\mu^2)^{1/2}} \frac{\partial \Psi}{\partial \lambda} \quad (2.10)$$

We linearize the equations by assuming that the streamfunction and temperature can be separated into a basic state plus a small perturbation,

$$\Psi = \bar{\Psi}(\mu, p) + \Psi' \quad (2.11)$$

$$T = \bar{T}(\mu, p) + T' \quad (2.12)$$

From (2.3), (2.4) and (2.9), we can derive the thermal wind relation,

$$\frac{\partial \bar{T}}{\partial \mu} = \frac{fa}{(1-\mu^2)^{1/2}} \frac{p}{R} \frac{\partial \bar{u}}{\partial p} \quad (2.13)$$

After neglecting nonlinear terms and dropping the primes, equations (2.1) to (2.5) give,

$$\left(\frac{\partial}{\partial t} + \frac{\bar{u}}{a(1-\mu^2)^{1/2}} \frac{\partial}{\partial \lambda} \right) \nabla^2 \Psi = - \frac{1}{a^2} \frac{\partial \Psi}{\partial \lambda} \left\{ 2\Omega - \frac{\partial^2}{\partial \mu^2} \left[\frac{(1-\mu^2)^{1/2}}{a} \bar{u} \right] \right\} \\ + f \frac{\partial \omega}{\partial p} - 2\Omega \frac{1-\mu^2}{a^2} \frac{\partial X}{\partial \mu} \quad (2.14)$$

$$\left(\frac{\partial}{\partial t} + \frac{\bar{u}}{a(1-\mu^2)^{1/2}} \frac{\partial}{\partial \lambda} \right) T = - \frac{f}{a(1-\mu^2)^{1/2}} \frac{\partial \Psi}{\partial \lambda} \frac{p}{R} \frac{\partial \bar{u}}{\partial p} + \sigma \omega \quad (2.15)$$

$$\nabla^2 \Phi = \nabla \cdot f \nabla \Psi \quad (2.16)$$

$$\frac{\partial \Phi}{\partial p} = - \frac{RT}{p} \quad (2.17)$$

To derive a single equation that is analogous to the β -plane quasigeostrophic potential vorticity equation, two approximations have to be adopted,

$$(1) \quad \text{neglect } 2\Omega \frac{1-\mu^2}{a^2} \frac{\partial X}{\partial \mu} \text{ in (2.14)}$$

$$(2) \quad \text{replace (2.16) by } \Phi = f \Psi$$

These approximations were introduced by Dickinson(1968) for the case of vertically propagating planetary waves. As pointed out by

Hollingsworth et al., the first one implies that the divergent part of the meridional wind is small in comparison with the geostrophic meridional wind, which is consistent with traditional quasigeostrophic scaling. With regard to the second one, Hollingsworth et al. show that errors introduced by this approximation are consistent with the usual quasigeostrophic approximation.

From approximation (2) and equation (2.17), we have

$$\tau = -\frac{f p}{R} \frac{\partial \Psi}{\partial p} \quad (2.18)$$

In terms of Ψ , (2.15) yields

$$\frac{\partial \omega}{\partial p} = -\left(\frac{\partial}{\partial t} + \frac{\bar{u}}{a(1-\mu^2)^{1/2}} \frac{\partial}{\partial \lambda} \right) \frac{\partial}{\partial p} \left(\frac{f p}{R \sigma} \frac{\partial \Psi}{\partial p} \right) + \frac{1}{a(1-\mu^2)^{1/2}} \frac{\partial \Psi}{\partial \lambda} \frac{\partial}{\partial p} \left(\frac{f p}{R \sigma} \frac{\partial \bar{u}}{\partial p} \right) \quad (2.19)$$

Substituting (2.19) into (2.14) with approximation (1), then we have the single governing equation on the sphere,

$$\begin{aligned} & \left(\frac{\partial}{\partial t} + \frac{\bar{u}}{a(1-\mu^2)^{1/2}} \frac{\partial}{\partial \lambda} \right) \left(\nabla^2 \Psi + \frac{\partial}{\partial p} \left(\frac{f^2 p}{R \sigma} \frac{\partial \Psi}{\partial p} \right) \right) \\ & + \frac{1}{a^2} \frac{\partial \Psi}{\partial \lambda} \left\{ 2\Omega - \frac{\partial^2}{\partial \mu^2} \left[\frac{(1-\mu^2)^{1/2} \bar{u}}{a} \right] - \frac{a}{(1-\mu^2)^{1/2}} \frac{\partial}{\partial p} \left(\frac{f^2 p}{R \sigma} \frac{\partial \bar{u}}{\partial p} \right) \right\} = 0 \end{aligned} \quad (2.20)$$

To check if this approximated equation would yield results in good agreement with those of Lorenz's model, Hollingsworth et al. applied both in a two-layer system to study the same baroclinic instability problem. The static stability is taken as a constant. The basic flow is a solid body rotation in the upper layer and a rest state in the lower layer.

Fig. 2.1, taken from Hollingsworth et al.(1976) fig. 1, shows the growth rates and phase speeds from both models as a function of the perturbation zonal wavenumber. We can see that, in general, the solutions of this approximated equation underestimate the growth rate and overestimate the phase speed. Nonetheless they are in very good agreement even at low wavenumbers where approximation (2) would give a larger error.

Fig. 2.2, taken from their fig. 2 and fig. 3, show the amplitude and phase of the fastest growing mode as a function of latitude for both models. We note that the amplitudes show little difference between these two models. As for phase, there are some differences near the equator. Since the amplitude is very small near the equator, these differences are not important.

These results indicate that those approximations that were introduced during the derivation of (2.20) do not have any significant effect on the nature of baroclinic instability on the sphere.

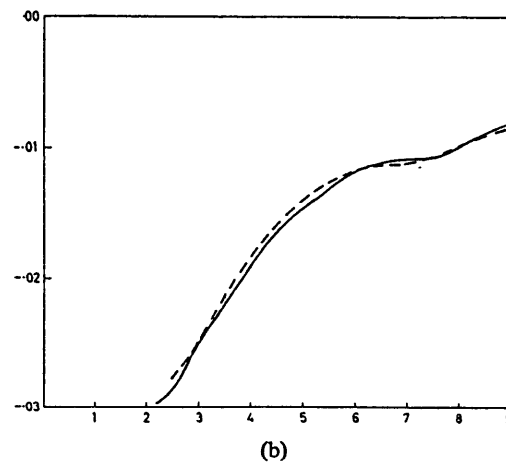
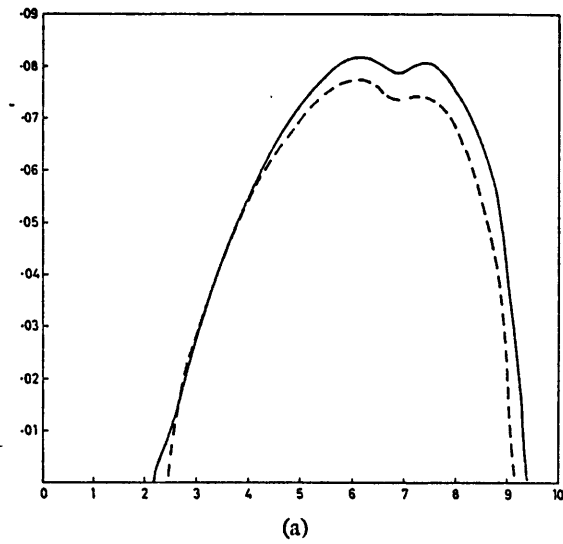


Fig. 2.1 The growth rates (a) and phase speeds (b) from Lorenz's model(solid) and approximated equation(dashes) as a function of zonal wavenumber, taken from fig.1 of Hollingsworth, Simmons and Hoskins(1976).

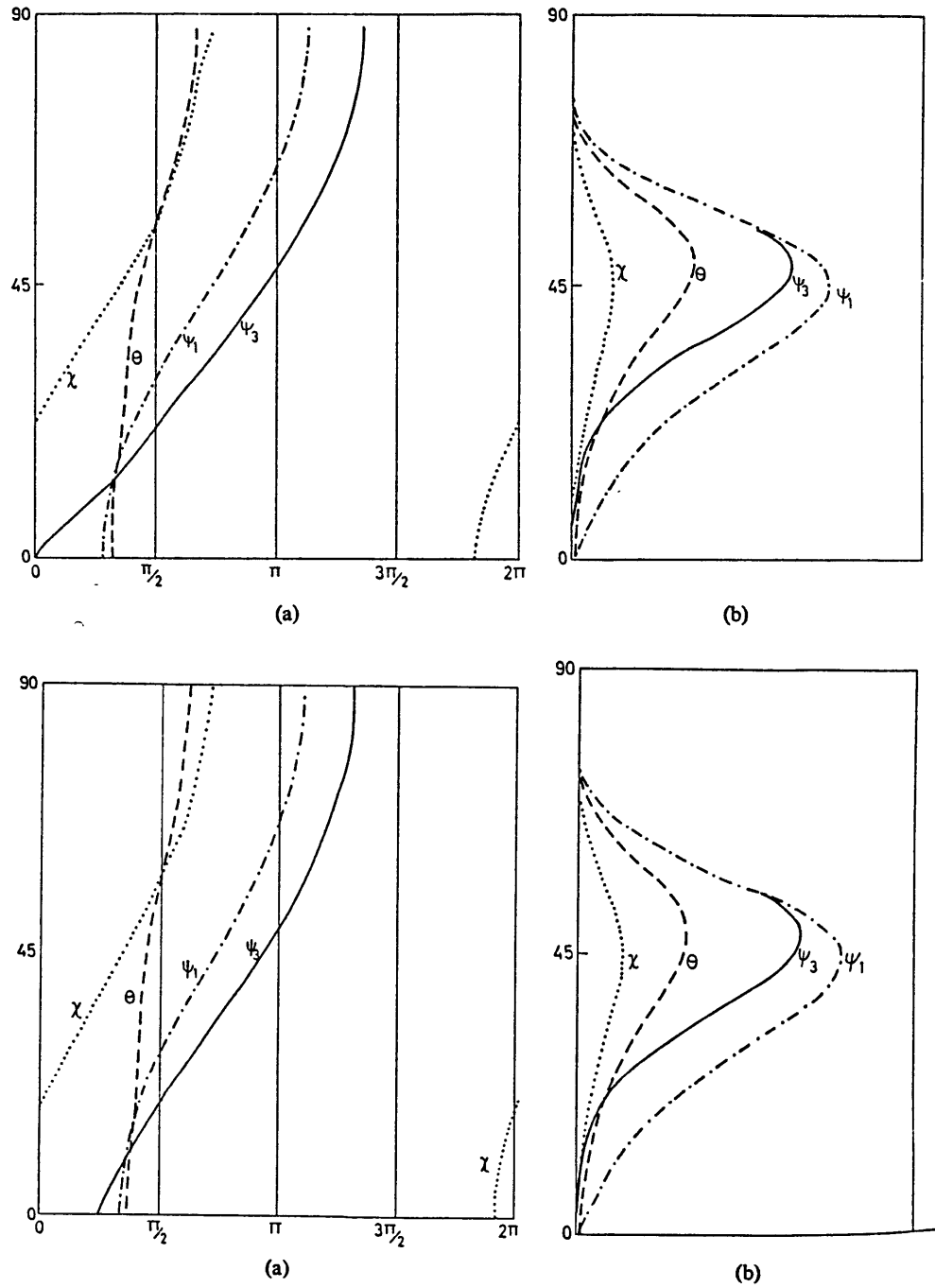


Fig. 2.2 The perturbation's phases (a) and amplitudes (b) as a function of latitude from both Lorenz's model(upper) and approximated equation(lower), taken from fig. 2 and fig. 3 of Hollingsworth, Simmons and Hoskins(1976).

To compare with β -plane analyses, we shall change (2.20) from pressure coordinates to height-coordinates and nondimensionalize the equation. We introduce

$$\begin{aligned} t &= \frac{a}{U_0} t^* \\ \bar{u} &= U_0 \bar{u}^* \\ z &= Hz^* \\ N^2 &= \frac{g}{\theta_s} \frac{\partial \theta_s}{\partial z} = N_0^2 N^{2*} \\ \nabla^2 &= \frac{1}{a^2} \nabla^{2*} \end{aligned}$$

where $()^*$ is a nondimensional quantity, H the scale height, U_0 the characteristic wind velocity, N^2 the Brunt-Vaisala frequency, N_0 the characteristic value of N , g the gravity, and θ_s the horizontal averaged potential temperature. With the aid of the hydrostatic equation, after dropping the stars, the resultant nondimensional equation is

$$\begin{aligned} & \left(\frac{\partial}{\partial t} + \frac{\bar{u}}{(1-\mu^2)^{1/2}} \frac{\partial}{\partial \lambda} \right) \left\{ \frac{1}{\rho} \frac{\partial}{\partial z} \left(\frac{\rho}{N^2} \frac{\partial \Psi}{\partial z} \right) + \frac{\epsilon^2}{\mu^2} \left[\frac{1}{1-\mu^2} \frac{\partial^2 \Psi}{\partial \lambda^2} + \frac{\partial}{\partial \mu} \left((1-\mu^2) \frac{\partial \Psi}{\partial \mu} \right) \right] \right\} \\ & + \frac{\partial \Psi}{\partial \lambda} \left\{ \frac{\beta_s}{\mu^2} - \frac{\epsilon^2}{\mu^2} \frac{\partial^2}{\partial \mu^2} [(1-\mu^2)^{1/2} \bar{u}] - \frac{1}{\rho(1-\mu^2)^{1/2}} \frac{\partial}{\partial z} \left(\frac{\rho}{N^2} \frac{\partial \bar{u}}{\partial z} \right) \right\} = 0 \end{aligned} \tag{ 2.21 }$$

The definitions of ϵ and β_s are

$$\varepsilon = \frac{N_0 H}{2\Omega a}, \quad \text{and} \quad \beta_s = \frac{N_0^2 H^2}{2\Omega a U_0} \quad (2.22)$$

It is easy to see that ε is proportional to the ratio between the radius of deformation and the radius of the sphere, while β_s is analogous to the β parameter on a β -plane. For the earth's atmosphere,

$$a \sim 6400 \text{ km}, \quad N_0^2 \sim 2 \times 10^{-4} \text{ sec}^{-2}, \quad \Omega \cong 7.29 \times 10^{-5} \text{ sec}^{-1}$$

$$H \sim 8 \text{ km}, \quad U_0 \sim 30 \text{ m sec}^{-1}$$

thus, $\varepsilon \cong 0.1212$ and $\beta_s \cong 0.457$. We can see that, in general, ε is a small quantity and β_s is approximately an order one quantity. If μ is replaced by μ_0 , then

$$\frac{\partial}{\partial x} = \frac{1}{(1-\mu_0^2)^{1/2}} \frac{\partial}{\partial \lambda}, \quad \text{and} \quad \frac{\partial}{\partial y} = \frac{1}{(1-\mu_0^2)^{1/2}} \frac{\partial}{\partial \mu},$$

and we note that the resulting equation is exactly the same as the nondimensional quasigeostrophic potential vorticity equation on a β -plane (from Pedlosky, 1987), that is

$$\begin{aligned}
& \left(\frac{\partial}{\partial t} + \bar{u} \frac{\partial}{\partial x} \right) \left\{ \frac{1}{\rho} \frac{\partial}{\partial z} \left(\frac{\rho}{N^2} \frac{\partial \Psi}{\partial z} \right) + S^2 \left(\frac{\partial^2 \Psi}{\partial x^2} + \frac{\partial^2 \Psi}{\partial y^2} \right) \right\} + \frac{\partial \Psi}{\partial x} \left\{ \beta - S^2 \frac{\partial^2 \bar{u}}{\partial y^2} \right. \\
& \quad \left. - \frac{1}{\rho} \frac{\partial}{\partial z} \left(\frac{\rho}{N^2} \frac{\partial \bar{u}}{\partial z} \right) \right\} = 0
\end{aligned}
\tag{2.23}$$

where

$$S = \frac{N_0 D}{2\Omega \mu_0 L}, \quad \text{and} \quad \beta = \frac{(1-\mu_0^2)^{1/2} N_0^2 D^2}{\mu_0^2 2\Omega a U_0}
\tag{2.24}$$

L and D are the perturbation's characteristic horizontal and vertical scales, and μ_0 the value of μ at 45° . Usually both S and β are order one quantities for synoptic scale disturbances. Therefore the main difference between these two equations is that the coefficients in (2.21) vary with latitude while those in (2.23) are constants.

Since (2.21) is analogous to (2.23), we can apply some results from β -plane theory to the sphere. One of them is the necessary condition for instability (Charney and Stern, 1962; Pedlosky, 1964a). We assume that the perturbation streamfunction has a normal mode solution,

$$\Psi = \psi(\mu, z) e^{i(k\lambda - ct)}$$

where c is the phase speed and may be complex, and k is the planetary zonal wavenumber, $k=1,2,3,\dots$, integer. Then we multiply

the equation resulting from (2.21) by $\rho\psi^*$, where ψ^* is a complex conjugate of ψ , and integrate over a meridional cross section. After integration by parts, we have

$$\begin{aligned}
& \int_0^1 \int_0^{z_t} \left\{ \frac{\rho\mu^2}{N^2} \left| \frac{\partial\psi}{\partial z} \right|^2 + \frac{\epsilon^2 k^2 |\psi|^2}{1-\mu^2} + \epsilon^2 (1-\mu^2) \left| \frac{\partial\psi}{\partial\mu} \right|^2 \right\} \partial z \partial\mu \\
&= \int_0^1 \int_0^{z_t} \frac{\rho |\psi|^2}{\frac{\bar{u}}{(1-\mu^2)^{1/2}} - c} \left\{ \beta_s - \epsilon^2 \frac{\partial^2}{\partial\mu^2} [(1-\mu^2)^{1/2} \bar{u}] - \frac{\mu^2}{\rho(1-\mu^2)^{1/2}} \frac{\partial}{\partial z} \left(\frac{\rho}{N^2} \frac{\partial \bar{u}}{\partial z} \right) \right\} \partial z \partial\mu \\
&+ \int_0^1 \left\{ \frac{\rho\mu^2}{N^2(1-\mu^2)^{1/2}} \frac{|\psi|^2}{\frac{\bar{u}}{(1-\mu^2)^{1/2}} - c} \frac{\partial \bar{u}}{\partial z} \right\}_0^{z_t} \partial\mu
\end{aligned} \tag{2.25}$$

The following boundary conditions have been applied to derive (2.25),

$$\Psi = 0 \quad \text{at } \mu=0, 1 \tag{2.26}$$

and

$$\left(\frac{\partial}{\partial t} + \frac{\bar{u}}{(1-\mu^2)^{1/2}} \frac{\partial}{\partial \lambda} \right) \frac{\partial \Psi}{\partial z} - \frac{1}{(1-\mu^2)^{1/2}} \frac{\partial \Psi}{\partial \lambda} \frac{\partial \bar{u}}{\partial z} = 0 \quad \text{at } z=0, z_t \tag{2.27}$$

If $z_t \rightarrow \infty$, the upper boundary condition is taken as $\Psi=0$, then there is no contribution from the integrated term at z_t . Since the left hand side of (2.25) is real, the imaginary part of the right hand side must

be zero. Therefore if there is instability, which means that c_i is positive, then we must require that

$$\int_0^1 \int_0^{z_t} \frac{\rho |\psi|^2}{\left| \frac{\bar{u}}{(1-\mu^2)^{1/2}} - c \right|^2} \left\{ \beta_s - \epsilon^2 \frac{\partial^2}{\partial \mu^2} [(1-\mu^2)^{1/2} \bar{u}] - \frac{\mu^2}{(1-\mu^2)^{1/2} \rho} \frac{\partial}{\partial z} \left(\frac{\rho}{N^2} \frac{\partial \bar{u}}{\partial z} \right) \right\} \partial z \partial \mu$$

$$+ \int_0^1 \left\{ \frac{\rho \mu^2}{N^2 (1-\mu^2)^{1/2}} \frac{|\psi|^2}{\left| \frac{\bar{u}}{(1-\mu^2)^{1/2}} - c \right|^2} \frac{\partial \bar{u}}{\partial z} \right\}_0^{z_t} \partial \mu = 0 \quad (2.28)$$

This is the necessary condition for instability on the sphere, which requires that one of the following conditions be met:

- (1). the basic state potential vorticity gradient changes sign within the domain;
- (2). the basic state potential vorticity gradient term is balanced by the boundary terms at $z=0$ and $z=z_t$;
- (3). the basic state potential vorticity gradient is zero and the boundary terms have opposite signs.

It is easy to see that these conditions are the same as those on a β -plane. We note that baroclinic instability of Charney's and Eady's Models require that either condition (2) or (3) be met. Since the form and properties of (2.21) and (2.23) closely resemble to each other, we can construct spherical models that are analogous to these two. Therefore we may be able to apply some of the methods from

those analytical studies of these two models to solve (2.21) analytically for certain kinds of basic flows. Moreover we can compare them with results from those studies to determine the effect of spherical geometry on baroclinic instability.

CHAPTER III

AN ANALOGUE OF EADY'S MODEL ON THE SPHERE

The simplest model that displays the baroclinic instability process was introduced by Eady(1949). The most significant feature in Eady's model is that there is no basic state potential vorticity gradient in the governing equation. As noted in the previous chapter, this feature requires that both upper and lower boundary terms be of opposite sign for instability to occur. Although the absence of the basic state potential vorticity gradient is unrealistic for application to the atmosphere, this model demonstrates the essential character of baroclinic instability. Therefore, in our analytic study of baroclinic instability on the sphere, we shall begin by investigating an analogue of the Eady problem.

To derive the analogue of Eady's model on the sphere, we shall assume that β_s is small. Furthermore, ρ and N^2 are taken as constants. The basic flow has constant vertical shear and has a solid body rotation for the meridional structure, i.e.,

$$\bar{u} = (1-\mu^2)^{1/2} z \quad (3.1)$$

We note that, in (2.21), the important basic flow terms are divided by $(1-\mu^2)^{1/2}$, therefore this flow can be seen as equivalent to meridionally uniform zonal flow on a β -plane or f -plane. Then we

look for the perturbation streamfunction that has a normal mode solution,

$$\Psi = \text{Re} \left\{ \frac{\psi(\mu, z)}{(1-\mu^2)^{1/2}} e^{ik(\lambda-ct)} \right\} \quad (3.2)$$

where $k=1,2,3,\dots$, is the zonal wavenumber. Since ϵ is small for the earth's atmosphere, it can be used as a perturbation parameter. We rescale k and β_s as

$$k = \epsilon^{-1} k_0 \quad \text{and} \quad \beta_s = \epsilon^2 \beta_0 \quad (3.3)$$

where k_0 and β_0 are taken as order one quantities. From (2.21), the resulting equation for ψ is

$$\frac{\partial^2 \psi}{\partial z^2} - \frac{k_0^2 - \epsilon^2}{\mu^2(1-\mu^2)} \psi + \epsilon^2 \frac{1-\mu^2}{\mu^2} \frac{\partial^2 \psi}{\partial \mu^2} + \frac{\epsilon^2}{\mu^2} \frac{\psi}{z-c} (\beta_0 + 2z) = 0 \quad (3.4)$$

It is noted that the basic state potential vorticity gradient is $O(\epsilon^2)$, except near the equator where μ approaches zero. Therefore, in general, it is very small in comparison with other terms in (3.4) and will not enter the leading order governing equation. The vertical boundary conditions are

$$(z-c) \frac{\partial \psi}{\partial z} - \psi = 0 \quad \text{at} \quad z = 0, 1 \quad (3.5)$$

These rigid boundaries are required for instability to occur at leading order. For the meridional boundary conditions, we just require that the streamfunction is zero at both the equator and pole,

$$\psi = 0 \quad \text{at } \mu = 0, 1 \quad (3.6)$$

We note that if the basic state potential vorticity gradient is neglected, then (3.4) does not contain a term that explicitly depends on both z and μ . If we assume separation of variables, it can be separated into two ordinary differential equations, one for the vertical structure of the perturbation and the other for the meridional structure. Therefore we assume that ψ can be separated as

$$\psi = \phi(z) \chi(\mu) \quad (3.7)$$

Substituting (3.7) into (3.4) and neglecting $O(\epsilon^2)$ terms, then we have,

$$\frac{\partial^2 \phi}{\partial z^2} - K^2 \phi = 0 \quad (3.8)$$

$$\frac{\partial^2 \chi}{\partial \mu^2} - \epsilon^{-2} Q(\mu) \chi = 0 \quad (3.9)$$

where K^2 is a separation function which may depend on μ . The definition of Q is

$$Q = \frac{\mu^2}{1-\mu^2} \left\{ \frac{k_0^2}{\mu^2(1-\mu^2)} - K^2 \right\} \quad (3.10)$$

From (3.5) and (3.7), the boundary conditions for ϕ are

$$(1-c) \frac{\partial \phi}{\partial z} - \phi = 0 \quad \text{at } z = 1 \quad (3.11)$$

and

$$c \frac{\partial \phi}{\partial z} + \phi = 0 \quad \text{at } z = 1 \quad (3.12)$$

As for χ , we have

$$\chi = 0 \quad \text{at } \mu = 0, 1 \quad (3.13)$$

If K is a constant, then (3.8), (3.11) and (3.12) are all independent of μ and are identical to those of Eady's model. The solution for (3.8) can readily be written as

$$\phi = A \cosh(Kz) + B \sinh(Kz) \quad (3.14)$$

Substituting (3.14) into (3.11) and (3.12), the boundary conditions for ϕ give

$$A\{(c-1)K \sinh K + \cosh K\} + B\{(c-1)K \cosh K + \sinh K\} = 0 \quad (3.15)$$

$$A + KcB = 0 \quad (3.16)$$

For A and B to have nontrivial solutions, we must require that the determinant of the coefficients in (3.15) and (3.16) vanish, which is

$$c^2 - c + \frac{\coth K}{K} - \frac{1}{K^2} = 0 \quad (3.17)$$

From (3.17), we can write c as a function of K ,

$$c = \frac{1}{2} \pm \frac{1}{K} \left\{ \left(\frac{K}{2} - \coth \frac{K}{2} \right) \left(\frac{K}{2} - \tanh \frac{K}{2} \right) \right\}^{1/2} \quad (3.18)$$

Since c is a constant, K has to be a constant also. We note that if there is instability then c must be complex and the imaginary part of c must be positive. This indicates that the radicand in (3.18) has to be negative. Since, for all K ,

$$\frac{K}{2} \geq \tanh \frac{K}{2}$$

the only possibility for the radicand being less than zero is that

$$\frac{K}{2} < \coth \frac{K}{2}$$

Therefore, for instability to occur, we must require that

$$K < K_c = 2.3994 \quad (3.19)$$

where K_c is the critical value for instability. We note that, except for K being unknown at this stage, (3.19) is exactly the same condition as that in Eady's problem.

To determine K , we have to find the solution for χ . Since ε is a small parameter, (3.9) is a standard WKB equation. From (3.10), we note that, if K is less than $2k_0$ then Q is positive everywhere.

Therefore the leading order asymptotic solution for χ can readily be written as (Bender and Orszag, 1978),

$$\chi \sim D_+ Q^{-1/4} \exp\left\{ \varepsilon^{-1} \int Q^{1/2} d\mu \right\} + D_- Q^{-1/4} \exp\left\{ -\varepsilon^{-1} \int Q^{1/2} d\mu \right\} \quad (3.20)$$

From (3.13), we know that (3.20) must be zero at both the equator and pole. This requires that both D_- and D_+ be zero, therefore there is no nontrivial solution for χ . On the other hand, if $K > 2k_0$, then

$$Q = \frac{\mu^2}{1-\mu^2} \left\{ \frac{k_0^2}{\mu^2(1-\mu^2)} - K^2 \right\} = 0, \quad \text{at } \mu = \mu_1 \text{ and } \mu = \mu_2 \quad (3.21)$$

where

$$\mu_1^2 = \frac{1}{2} + \frac{1}{2} \left(1 + 4 \left(\frac{k_0}{K} \right)^2 \right)^{1/2} \quad (3.22)$$

and

$$\mu_2^2 = \frac{1}{2} - \frac{1}{2} \left(1 + 4 \left(\frac{k_0}{K} \right)^2 \right)^{1/2} \quad (3.23)$$

We note that, for this particular basic flow, the squares of μ_1 and μ_2 are symmetrical about 45° latitude. Since $Q=0$ at these two latitudes, equation (3.9) becomes a standard two-turning-point WKB problem. For $\mu > \mu_1$ or $\mu < \mu_2$, Q is positive, therefore the solution for χ is an exponential function. For $\mu_2 < \mu < \mu_1$, Q is negative, the solution is an oscillatory function. While near μ_1 or μ_2 , Q is approaching zero, and the WKB solution does not exist. The solutions in these regions are approximated by Airy functions. To match two one-turning-point solutions in the region $\mu_2 < \mu < \mu_1$, a connection condition must be satisfied,

$$\int_{\mu_1}^{\mu_2} (-Q)^{1/2} d\mu = \varepsilon \left(n - \frac{1}{2} \right) \pi \quad (3.24)$$

where $n= 1, 2, 3, \dots$, is a positive integer. Then the solution for χ in each region can be written as

$$\chi \sim Q^{-1/4} \exp \left\{ -\varepsilon^{-1} \int_{\mu_1}^{\mu} Q^{1/2} d\mu \right\}, \quad \text{for } \mu_1 + O(\varepsilon^{2/3}) < \mu \leq 1$$

$$\begin{aligned} \chi &\sim 2\sqrt{\pi} (\epsilon a_1)^{-1/6} A_1 \{ \epsilon^{-2/3} a_1^{1/3} (\mu - \mu_1) \} \quad \text{for } \mu_1 - O(\epsilon^{2/3}) \leq \mu \leq \mu_1 + O(\epsilon^{2/3}) \\ \chi &\sim 2(-Q)^{-1/4} \sin\left(\epsilon^{-1} \int_{\mu}^{\mu_1} (-Q)^{1/2} d\mu + \frac{\pi}{4}\right) \quad \text{for } \mu_2 + O(\epsilon^{2/3}) < \mu < \mu_1 + O(\epsilon^{2/3}) \\ \chi &\sim (-1)^{n+1} 2\sqrt{\pi} (\epsilon a_2)^{-1/6} A_1 \{ \epsilon^{-2/3} a_2^{1/3} (\mu - \mu_2) \} \quad \mu_2 - O(\epsilon^{2/3}) \leq \mu \leq \mu_2 + O(\epsilon^{2/3}) \\ \chi &\sim (-1)^{n+1} Q^{-1/4} \exp\left\{-\epsilon^{-1} \int_{\mu}^{\mu_2} Q^{1/2} d\mu\right\}, \quad \text{for } 0 \leq \mu < \mu_2 - O(\epsilon^{2/3}) \end{aligned} \quad (3.25)$$

where

$$a_m = \frac{dQ}{d\mu}, \quad \text{at } \mu = \mu_m, \quad m = 1, 2$$

From (3.24) and (3.25), we can see that n is the meridional wavenumber. For given n and k_0 , K is uniquely determined by (3.24). Therefore, from (3.18), we can determine c . Since K must be less than K_c for instability to occur and must be greater than $2k_0$ for χ to have a nontrivial solution, the unstable range of K is $2k_0 < K < K_c$. We note that there is a shortwave cutoff for instability as in Eady's model. Moreover as n increases then, from (3.25), K must also increase. Hence for each n there is a different cutoff zonal wavenumber for instability.

From (3.16), we can find B in terms of A, which can not be determined by linear theory. Therefore, aside from this constant, the vertical structure of the perturbation can be written as

$$\phi = \cosh(Kz) - \frac{\sinh(Kz)}{Kc} \quad (3.26)$$

If the perturbation is unstable, $c=c_r+c_i$ and $c_i \neq 0$, the amplitude and phase of ϕ are

$$|\phi| = \left\{ \left(\cosh(Kz) - \frac{c_r \sinh(Kz)}{K|c|^2} \right)^2 + \left(\frac{c_i \sinh(Kz)}{K|c|^2} \right)^2 \right\}^{1/2} \quad (3.27)$$

and

$$\alpha = \tan^{-1} \left\{ \frac{c_i \sinh(Kz)}{K|c|^2 \cosh(Kz) - c_r \sinh(Kz)} \right\} \quad (3.28)$$

Since K is a constant, $|\phi|$ and α are independent of latitude. For given K, ϕ is the same as that in Eady's model. The spherical geometry shows no effect on the vertical structure of the perturbation. As for the meridional structure, since Q is real, from (3.25), χ is also a real function. There is no meridional variation of phase.

From the solutions of ϕ and χ , we can write the perturbation streamfunction as

$$\Psi = \frac{|\phi| |\chi| e^{kc_i t}}{(1-\mu^2)^{1/2}} \operatorname{Re} \left\{ e^{i\alpha} e^{ik(\lambda - c_i t)} \right\} \quad (3.29)$$

Hence the meridional eddy heat flux can be expressed as

$$\overline{vT} = \frac{1}{(1-\mu^2)^{1/2}} \overline{\frac{\partial \Psi}{\partial \lambda} \frac{\partial \Psi}{\partial z}} = \frac{kc_i e^{2kc_i t}}{2(1-\mu^2)^{3/2} |c|^2} |\chi|^2 \quad (3.30)$$

We can see that the heat flux depends on c_i . If the wave is neutral, $c_i=0$, there is no heat flux. If the wave is unstable, then it will transfer heat poleward. Furthermore this heat flux is independent of height and is proportional to $|\chi|^2$. As for the momentum flux, since the perturbation does not have meridional phase variation, it is identically zero,

$$\overline{uv} = \overline{\frac{\partial \Psi}{\partial \lambda} \frac{\partial \Psi}{\partial \mu}} = 0 \quad (3.31)$$

In the following, we shall present some results from above solutions. The basic state parameters, U_0 , N_0 , Ω , a and H , are the same as in the previous chapter, therefore $\epsilon=0.1212$. Fig. 3.1 shows the meridional structure of the basic flow at upper boundary as a function of latitude. This is a cosine profile with the maximum velocity at the equator and zero at the pole.

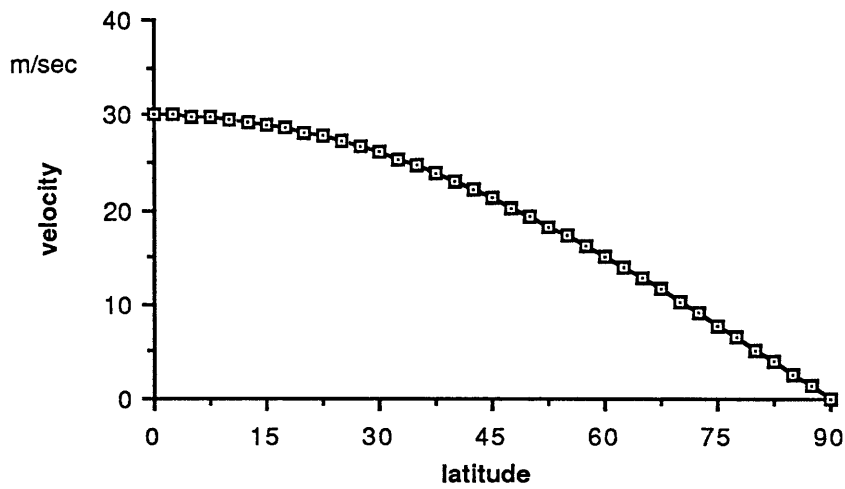


Fig. 3.1. The meridional structure of the basic flow as a function of latitude at $z=1$.

In fig. 3.2, we show the growth rate as a function of zonal wavenumber k for each meridional wavenumber n , $n=1,2,3$. It is noted that, for each n , there is a critical zonal wavenumber k_c . When $k < k_c$, the wave is unstable, while for $k \geq k_c$, there is no instability. Moreover, as n increases, k_c decreases. Comparing the growth rates for each n , we note that the lowest meridional mode has the largest growth rate. The most unstable wave is $k=6$, which has a zonal scale about 4500 km. This is very similar to the zonal scale of the most unstable wave in Eady's model. For given n , the scale of the zonal wave that has the maximum growth rate shifts toward longer scales as n increases.

Fig. 3.3 shows the steering level, which is $z_s=c_r$, as a function of k for $n=1,2,3$. We note that, for unstable waves, the steering levels are all located at mid level. This also implies that all unstable waves travel at the mean speed of the basic flow, which is exactly the same as in Eady's model. For neutral waves, depending upon the sign in (3.18), the steering level approaches either the upper or lower boundary as k increases.

Fig. 3.4 shows the variation of $|\phi|$ and α with height for the most unstable wave, $k=6$ and $n=1$. We can see that $|\phi|$ is nearly symmetrical about mid level where the minimum amplitude is located. The maxima of $|\phi|$ are located at both upper and lower boundaries. As for α , it is an increasing function of height. This implies that the phase of the wave tilts upward and westward with height, which indicates the conversion of available potential energy of the basic state to the energy of the perturbation. As mentioned in chapter i, for instability to occur, the absence of the basic state potential vorticity gradient requires that the vertical scale of the unstable wave is the same as the basic flow. Since ϕ is independent of μ , the vertical structure of the perturbation in any meridional location is the same as that shown in the figure.

In fig. 3.5, we show the amplitude of the most unstable wave as a function of latitude. It is noted that the amplitude peaks near 45° and decays toward both the equator and pole. Since the basic potential vorticity gradient, which will become large near the equator, is neglected, the amplitude near the equator does not decay

as rapidly as it might otherwise. There is no phase variation of the meridional structure.

From the above results we note that this particular case on the sphere is almost identical to Eady's model. The absence of the basic state potential vorticity gradient causes the governing equation to become a separable differential equation. Therefore the spherical geometry only plays the same role as the plane geometry in determining the meridional structure of the perturbation. It does not have any significant effect on the behavior of the unstable baroclinic wave. Furthermore, since we neglect the basic state potential vorticity gradient in (3.4), the amplitude of the perturbation in low latitudes may be too large and the eddy momentum flux does not exist in this case. Therefore, to examine the effect of spherical geometry on baroclinic instability, we should not neglect the basic state potential vorticity gradient, especially the β_s term, in the governing equation.

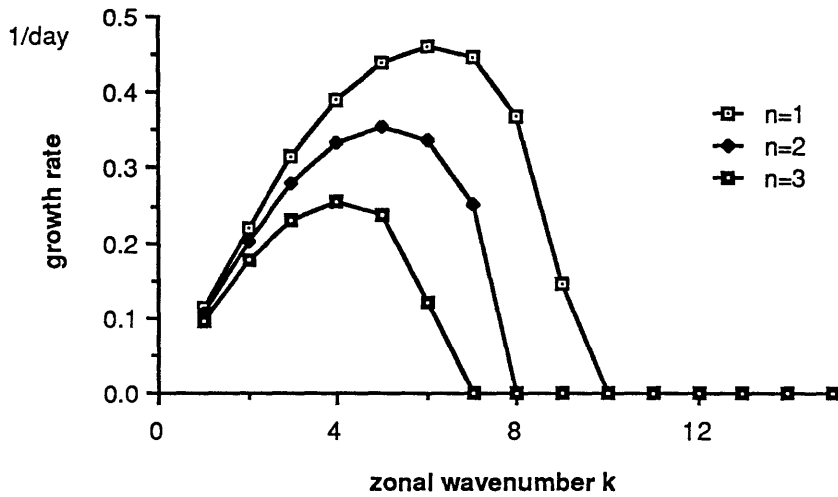


Fig. 3.2. The growth rate as a function of zonal wave number for each meridional wave number n , $n=1,2,3$.

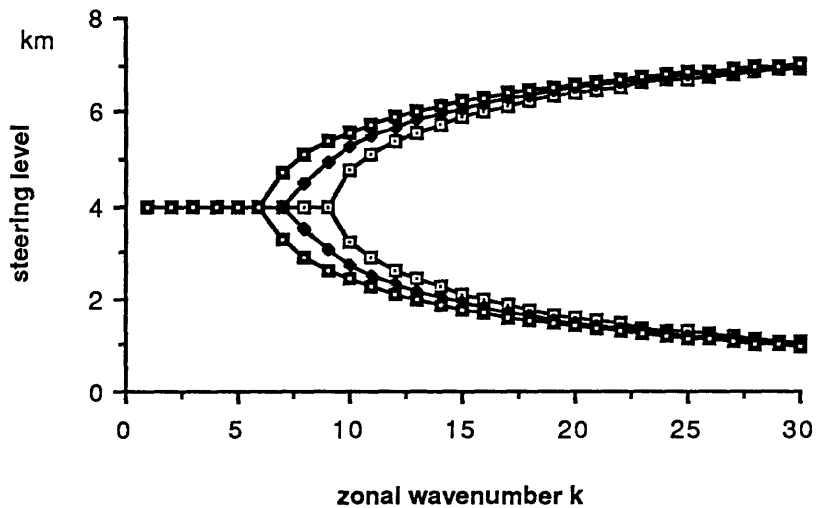


Fig. 3.3. As in fig. 2.2, except for the steering level.

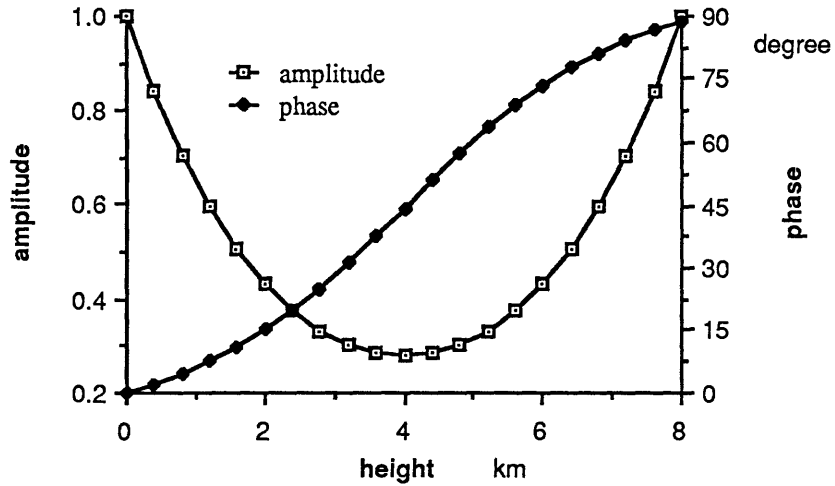


Fig. 3.4. The amplitude and phase of the most unstable wave, $k=6$ and $n=1$, as a function of height.

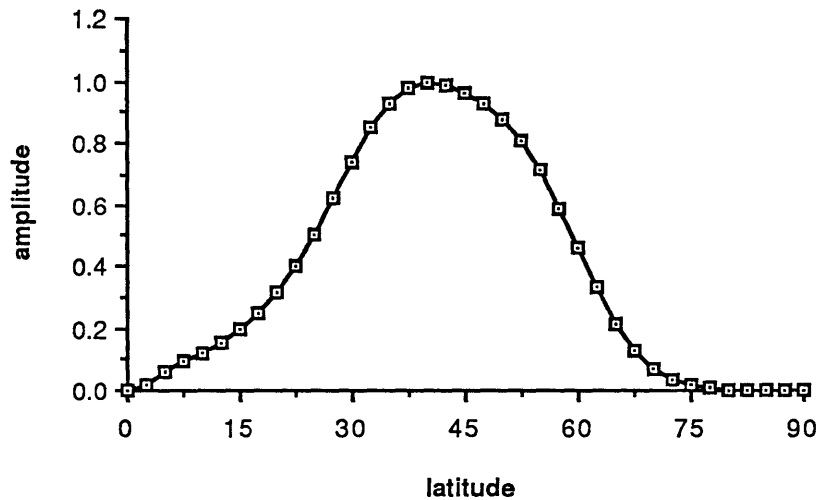


Fig. 3.5. The amplitude of the most unstable wave as a function of latitude.

CHAPTER IV

AN ANALOGUE OF CHARNEY'S MODEL ON THE SPHERE

From the previous chapter we note that, without the basic state potential vorticity gradient, there is no significant difference between the baroclinic instability problem on the sphere and that of Eady's problem. As discussed in chapter i, Charney's model, which includes the β -effect, has been used in many studies to investigate baroclinic instability on a β -plane. Therefore, to find out the effect of spherical geometry and to develop a proper procedure to solve the baroclinic instability problem on the sphere analytically, we shall study an analogue of Charney's model.

In this chapter, we take β_s as an order one quantity. As in Charney's model, the static stability, N^2 , is assumed to be a constant. The basic state density is an exponentially decreasing function of height,

$$\rho = e^{-z}$$

The basic zonal flow remains the same as that in chapter iii, which is a linear function of height multiplied by a solid body rotation,

$$\bar{u} = (1-\mu^2)^{1/2}z \tag{ 4.1 }$$

As mentioned before, this is equivalent to y independent zonal flow on a β -plane. We assume that the perturbation streamfunction has a normal mode solution,

$$\Psi = \text{Re} \left\{ \frac{\psi(\mu, z) e^{ik(\lambda - ct)}}{(1 - \mu^2)^{1/2}} \right\} \quad (4.2)$$

Substituting (4.2) into (2.21), the resulting governing equation for ψ is

$$\frac{\partial^2 \psi}{\partial z^2} - \frac{\partial \psi}{\partial z} - \varepsilon^2 \frac{k^2 - 1}{\mu^2(1 - \mu^2)} \psi + \varepsilon^2 \frac{1 - \mu^2}{\mu^2} \frac{\partial^2 \psi}{\partial \mu^2} + \frac{\psi}{z - c} \left\{ \frac{\beta_s}{\mu^2} + 1 + \frac{\varepsilon^2 2z}{\mu^2} \right\} = 0 \quad (4.3)$$

Since there is density variation with height, besides the β_s term and the barotropic term, a baroclinic term which has the value of unity is also present in the basic state potential vorticity gradient. We note that, except for the explicit meridional variations, equation (4.3) is very similar to the governing equation of Charney's problem.

The meridional boundary conditions, which require that the perturbation streamfunction be zero at both the equator and pole, are the same as (3.6),

$$\psi = 0, \quad \text{at } \mu = 0, 1 \quad (4.4)$$

We assume a horizontal rigid surface at the ground, therefore the lower boundary condition can be written as

$$c \frac{\partial \psi}{\partial z} + \psi = 0 \quad (4.5)$$

Due to the existence of the basic state potential vorticity gradient, the necessary condition for instability allows us to replace the upper rigid plane with a boundary condition at infinity, which is,

$$\psi = 0, \quad \text{as } z \rightarrow \infty \quad (4.6)$$

We note that the vertical boundary conditions, (4.5) and (4.6), do not explicitly depend on μ for this particular basic flow and are identical to those of Charney's model.

To examine the effect of spherical geometry on baroclinic instability, we need to be able to determine the properties of the unstable baroclinic waves as explicitly as possible. Although there were many studies of Charney's problem in the past(Charney, 1947; Kuo, 1952, 1973; Lindzen and Rosenthal, 1981; Branscome, 1983, etc.), most of these studies indicated that the analytic solutions of Charney's model are complicated and need a lot of numerical calculations to determine the properties of the unstable baroclinic waves. Furthermore, due to the presence of the basic state potential vorticity gradient, (4.3) depends on both latitude and height and is

more difficult to solve than Charney's problem. Therefore, we have to simplify the problem.

Branscome(1983) introduced a shortwave approximation to study Charney's problem. As discussed in chapter i, by using this shortwave approximation, the basic state potential vorticity gradient did not enter the leading order equation. Therefore, the solutions were easier to find and simpler. Moreover, the properties of the unstable baroclinic waves could be determined without any complicated calculations. Though these perturbation solutions are not valid for the whole zonal wave spectrum, in comparison with the exact solution, they do give reasonable results even at synoptic scale wavenumbers.

We shall apply this approximation to simplify the problem by assuming that the perturbation's zonal wavenumber is $O(\varepsilon^{-2})$. Since the short waves are shallow, we rescale k , z and c as

$$k = \varepsilon^{-2}k_0, \quad z = \varepsilon \zeta \quad \text{and} \quad c = \varepsilon c' \quad (4.7)$$

where k_0 , ζ and c' are taken as order one quantities. In terms of ζ , after dropping the prime of c' , (4.3) and (4.5) become,

$$\frac{\partial^2 \psi}{\partial \zeta^2} - \varepsilon \frac{\partial \psi}{\partial \zeta} - \frac{k_0^2 - \varepsilon^4}{\mu^2(1-\mu^2)} \psi + \varepsilon^4 \frac{1-\mu^2}{\mu^2} \frac{\partial^2 \psi}{\partial \mu^2} + \frac{\varepsilon \psi}{\zeta - c} \left\{ \frac{\beta_s}{\mu^2} + 1 + \frac{\varepsilon^2 \zeta}{\mu^2} \right\} = 0 \quad (4.8)$$

$$c \frac{\partial \psi}{\partial \zeta} + \psi = 0 \quad (4.9)$$

We note that the basic state potential vorticity gradient is $O(\varepsilon)$ smaller than other terms in (4.8), therefore it does not appear in the leading order perturbation equation. Because of the existence of the β_s term, which depends on both μ and ζ , we can not directly apply separation of variables to (4.8) as in chapter iii. Instead, we shall apply a two-scale formalism to the meridional variable to separate the perturbation's fast variation meridional structure from the vertical structure. We assume that ψ has two different meridional scales and can be written as

$$\psi = \phi(\mu, \zeta) \chi(\eta) \quad (4.10)$$

where η is the fast variation meridional scale. In order to retain the μ variations to lowest order so that the boundary conditions in μ can be satisfied, the meridional variations must be even more rapid than in the Eady problem, and we must define

$$\eta = \varepsilon^{-2} \mu \quad (4.11)$$

χ is the principle meridional structure of the perturbation and ϕ is the vertical structure with slow meridional variation. Furthermore, we assume that the governing equation for χ is

$$\frac{\partial^2 \chi}{\partial \eta^2} - Q^2 \chi = \varepsilon^4 \frac{\partial^2 \chi}{\partial \mu^2} - Q^2 \chi = 0 \quad (4.12)$$

where Q is an unknown function of μ and will be determined by solving the vertical structure equation. From (4.10) and (4.12), the μ derivative term in (4.8) becomes

$$\frac{\partial^2 \psi}{\partial \mu^2} = \varepsilon^{-4} \left\{ Q^2 \phi + \varepsilon^2 \frac{2}{\chi} \frac{\partial \chi}{\partial \eta} \frac{\partial \phi}{\partial \mu} + \varepsilon^4 \frac{\partial^2 \phi}{\partial \mu^2} \right\} \chi \quad (4.13)$$

Substituting (4.10) and (4.13) into (4.8), we have the governing equation for ϕ , which is

$$\begin{aligned} \frac{\partial^2 \phi}{\partial \zeta^2} - \varepsilon \frac{\partial \phi}{\partial \zeta} - K^2 \phi + \frac{\varepsilon^4 \phi}{\mu^2(1-\mu^2)} + \varepsilon^2 \frac{1-\mu^2}{\mu^2} \left\{ \frac{2}{\chi} \frac{\partial \chi}{\partial \eta} \frac{\partial \phi}{\partial \mu} + \varepsilon^2 \frac{\partial^2 \phi}{\partial \mu^2} \right\} \\ + \frac{\varepsilon \phi}{\zeta - c} \left(b + \frac{\varepsilon^3 2\zeta}{\mu^2} \right) = 0 \end{aligned} \quad (4.14)$$

where we define that,

$$K^2 = \frac{k_0^2}{\mu^2(1-\mu^2)} - \frac{1-\mu^2}{\mu^2} Q^2 \quad (4.15)$$

and

$$b = \frac{\beta_s}{\mu^2} + 1 \quad (4.16)$$

Since Q is unknown, K is also an unknown function of μ . b is the leading order basic state potential vorticity gradient. We note that

(4.12) is a standard WKB equation and its asymptotic solution can be written as

$$\chi \sim \exp\left\{ \varepsilon^{-2} \int^{\mu} \sum_{n=0}^{\infty} \varepsilon^{2n} q_n d\tau \right\} \quad (4.17)$$

where

$$q_0^2 = Q^2, \quad 2q_0 q_1 + \frac{dq_0}{d\mu} = 0, \quad (4.18)$$

and

$$2q_0 q_n + \frac{dq_{n-1}}{d\mu} + \sum_{j=1}^{n-1} q_j q_{n-j}, \quad n \geq 2. \quad (4.19)$$

With (4.17), the η derivative term in (4.14) can be calculated as

$$\frac{1}{\chi} \frac{\partial \chi}{\partial \eta} = \sum_{n=0}^{\infty} \varepsilon^{2n} q_n \quad (4.20)$$

Therefore ϕ does not really depend on χ or η . If Q is not an order one quantity somewhere in the meridional domain, then this two-scale expansion will not be valid near that location. We need to apply a local expansion to solve (4.8) in that region.

From (4.6), (4.9) and (4.10), the boundary conditions for ϕ are,

$$c \frac{\partial \phi}{\partial \zeta} + \phi = 0, \quad \text{at } \zeta = 0 \quad (4.21)$$

and

$$\phi = 0 \quad \text{as } \zeta \rightarrow \infty \quad (4.22)$$

For χ , the boundary conditions are

$$\chi = 0, \quad \text{at } \mu = 0, 1 \quad (4.23)$$

We note that there are two unknowns, K and c , in these equations. By requiring that (4.21) and (4.22) be satisfied by the solution of (4.14), we can find K as a function of c . Once K is known, from (4.15), we can determine Q . Since K is a function of c , Q will also depend on c . Then c is determined by requiring that χ meet the boundary condition (4.23).

In the following, we shall apply a perturbation method to solve (4.14). We assume that

$$\phi = \sum_{n=0}^{\infty} \varepsilon^n \phi_n, \quad c = \sum_{n=0}^{\infty} \varepsilon^n c_n, \quad \text{and} \quad K = \sum_{n=0}^{\infty} \varepsilon^n K_n \quad (4.24)$$

Since, if c_0 is real there is a singularity at $\zeta = c_0$, we need an inner equation to properly describe the behavior of ϕ near this layer. We introduce an inner variable,

$$\xi = \varepsilon^{-1}(\zeta - c_0) \quad (4.25)$$

In terms of ξ , (4.14) becomes

$$\frac{\partial^2 \phi^i}{\partial \xi^2} - \varepsilon^2 \frac{\partial \phi^i}{\partial \xi} - \varepsilon^2 K^2 \phi^i + \frac{\varepsilon^2 b \phi^i}{\xi - c_1} \left\{ 1 + \frac{\varepsilon c_2}{\xi - c_1} \right\} + O(\varepsilon^4) = 0 \quad (4.26)$$

where ϕ^i is the inner solution for the vertical structure and can be expressed in the same form as ϕ in (4.24).

The leading order perturbation equations and boundary conditions are,

$$\frac{\partial^2 \phi_0}{\partial \zeta^2} - K_0^2 \phi_0 = L_0 \phi_0 = 0 \quad (4.27)$$

$$c_0 \frac{\partial \phi_0}{\partial \zeta} + \phi_0 = 0, \quad \text{at } \zeta = 0 \quad (4.28)$$

$$\phi_0 = \phi_1 = \phi_2 = \dots = 0, \quad \text{as } \zeta \rightarrow \infty \quad (4.29)$$

and

$$\frac{\partial^2 \phi_0^i}{\partial \xi^2} = L_0^i \phi_0^i = 0 \quad (4.30)$$

We note that these equations do not explicitly depend on μ . After satisfying the upper boundary condition, the solution of (4.27) can be written as

$$\phi_0 = A_0 e^{-K_0 (\zeta - c_0)} \quad (4.31)$$

where A_0 is a constant. We lose no generality by taking A_0 to be independent of μ , because any such dependence can be absorbed in χ . The lower boundary condition (4.28) requires that

$$K_0 = \frac{1}{c_0} \quad (4.32)$$

Since c_0 is a constant, K_0 has to be a constant also. This implies that ϕ_0 is just a simple exponentially decreasing function of height and does not vary with latitude. Furthermore, since K_0 is a constant, the leading order vertical scale does not vary with latitude. The solution of (4.30) is $A\xi+B$. Since, in terms of ξ , the leading order of (4.31) is just A_0 , therefore $A=0$ and $B=A_0$, and the leading order inner solution is

$$\phi_0^i = A_0 \quad (4.33)$$

Except for the fact that K_0 is unknown at this stage, these leading order solutions are the same as those of Branscome(1983).

The first order equations for ϕ and ϕ^i can be written as

$$L_0 \phi_1 = \frac{\partial \phi_0}{\partial \zeta} + 2K_0 K_1 \phi_0 - \frac{b\phi_0}{\zeta - c_0} = L_1 \phi_0 \quad (4.34)$$

and

$$L_0^i \phi_1^i = 0 \quad (4.35)$$

The lower boundary condition for ϕ_1 is

$$c_0 \frac{\partial \phi_1}{\partial \zeta} + \phi_1 = -c_1 \frac{\partial \phi_0}{\partial \zeta} \quad (4.36)$$

The only difference between these equations and those of Branscome(1983) is the existence of the $2K_0K_1$ term in (4.34). From Hildebrand(1976), the particular solution of ϕ_1 can be found as

$$\phi_1 = e^{-K_0(\zeta-c_0)} \int_{\zeta}^{\infty} e^{2K_0(\zeta-c_0)} \left\{ \int_{\zeta}^{\infty} e^{-K_0(x-c_0)} L_1 \phi_0 dx \right\} d\zeta \quad (4.37)$$

After integration, the solution for ϕ_1 is

$$\begin{aligned} \phi_1 = & A_0 e^{-K_0(\zeta-c_0)} \left\{ \left(\frac{1}{2} - K_1 \right) \zeta \right. \\ & \left. + \frac{b}{2K_0} \left[e^{2K_0(\zeta-c_0)} E_1(2K_0(\zeta-c_0)) + \ln K_0(\zeta-c_0) \right] \right\} \end{aligned} \quad (4.38)$$

where the definition of $E_1(x)$ is(Abramowitz and Stegun, 1964)

$$E_1(x) = \int_x^{\infty} \frac{e^{-t}}{t} dt, \quad x \neq 0 \quad (4.39)$$

If x is negative, then

$$E_1(x) = -E_1(-x) \pm i\pi, \quad x < 0 \quad (4.40)$$

and

$$E_1(x) = - \int_{-x}^{\infty} \frac{e^{-t}}{t} dt, \quad x > 0 \quad (4.41)$$

Therefore, if $\zeta < c_0$, ϕ_1 will be complex. This feature is due to the existence of the basic state potential vorticity gradient. Since we look for instability, we shall only choose the positive sign in (4.40). The lower boundary condition yields

$$K_1 = \frac{1}{2} + be^{-2}E_1(-2) - K_0^2 c_1 = \frac{1}{2} - K_0^2 c_1 - be^{-2}(E_1(2) - i\pi) \quad (4.42)$$

K_1 is a complex function. Since b varies with $1/\mu^2$, K_1 also varies with $1/\mu^2$. In terms of ξ , the first two orders of ϕ can be approximated as

$$\begin{aligned} \phi_0 + \varepsilon\phi_1 \approx A_0 \left\{ 1 + \varepsilon \left\{ -K_0 \xi + \frac{1}{K_0} \left(\frac{1}{2} - K_1 \right) - \frac{b}{2K_0} (E_0 + \ln 2) \right\} \right. \\ \left. + \varepsilon^2 \left\{ \frac{K_0^2 \xi^2}{2} - \varepsilon b \xi \left(\ln \varepsilon K_0 \xi + \frac{E_0 + \ln 2 - 1}{2} \right) \right\} \right\} \end{aligned} \quad (4.43)$$

where $E_0 = 0.5772\dots$, is Euler's constant. It is noted that if $\xi < 0$, then

$$\ln \xi = \ln(-\xi) - i\pi \quad (4.44)$$

The general solution of (4.35) is also $A\xi+B$. After matching with (4.43), we can determine A and B. Therefore the first order inner solution is

$$\phi_1^i = A_0 \left\{ -K_0 \xi + \frac{1}{K_0} (K_0^2 c_1 - b e^{-2} E_1(-2) - \frac{b}{2} (E_0 + \ln 2)) \right\} \quad (4.45)$$

Since (4.38) and (4.45) depend on b, they will vary with latitude. Except for b being a function of μ , these solutions are virtually identical to those of Branscome(1983).

The second order perturbation equations for ϕ and ϕ^i are

$$\begin{aligned} L_0 \phi_2 &= L_1 \phi_1 + (2K_0 K_2 + K_1^2) \phi_0 - \frac{1-\mu^2}{\mu^2} \frac{2}{\chi} \frac{\partial \chi}{\partial \eta} \frac{\partial \phi_0}{\partial \mu} - \frac{c_1 b \phi_0}{(\zeta - c_0)^2} \\ &= L_1 \phi_1 + L_2 \phi_0 \end{aligned} \quad (4.46)$$

and

$$L_0^i \phi_2^i = \frac{\partial \phi_0^i}{\partial \xi} + K_0^2 \phi_0^i - \frac{b \phi_0^i}{\xi - c_1} \quad (4.47)$$

The lower boundary condition for ϕ is

$$c_0 \frac{\partial \phi_2}{\partial \zeta} + \phi_2 = -c_1 \frac{\partial \phi_1}{\partial \zeta} - c_2 \frac{\partial \phi_0}{\partial \zeta} \quad (4.48)$$

Because we are mainly interested in determining c_2 , there is no need to find a solution for (4.46). Instead, we require that ϕ_2 remain finite. Therefore we multiply (4.46) by a homogeneous solution and integrate it from $\zeta=0$ to $\zeta \rightarrow \infty$,

$$\int_0^{\infty} e^{-K_0(\tau-c_0)} L_0 \phi_2 d\tau = \int_0^{\infty} e^{-K_0(\tau-c_0)} (L_1 \phi_1 + L_2 \phi_0) d\tau \quad (4.49)$$

After integration by parts and applying the upper and lower boundary conditions, (4.49) gives the solvability condition, which is,

$$eK_0 \left\{ c_1 \frac{\partial \phi_1}{\partial \zeta} + c_2 \frac{\partial \phi_0}{\partial \zeta} \right\}_{\zeta=0} = \int_0^{\infty} (L_1 \phi_1 + L_2 \phi_0) e^{-K_0(\tau-c_0)} d\tau \quad (4.50)$$

To satisfy this condition, we must require that

$$\begin{aligned} 2K_0 K_2 + K_1^2 = b^2 e^{-2} F - 2K_0^3 c_2 + 3K_0^4 c_1^2 - 2K_0^2 c_1 b e^{-2} E_1(-2) - K_0^2 c_1 \\ - b(1 + e^{-2} E_1(-2)) - b^2 e^{-2} E_1(-2) \{ 4e^{-2} E_1(-2) + 2 - i\pi \} \end{aligned} \quad (4.51)$$

where

$$F = \int_0^{\infty} \frac{d\tau}{\tau - c_0} \left\{ E_1(2K_0(\tau - c_0)) + e^{-2K_0(\tau-c_0)} \ln K_0(\tau - c_0) \right\} \quad (4.52)$$

Since ϕ_0 is independent of μ , the η derivative term in (4.46) is not present in (4.51). The solution of (4.47), after matching with (4.43), is

$$\begin{aligned} \phi_2^i = A_0 \left\{ \frac{K_0^2 \xi^2}{2} - b(\xi - c_1) \ln K_0(\xi - c_1) \right. \\ \left. + \frac{b\xi}{2} (2 - E_0 - \ln 2) \right\} + \text{constant.} \end{aligned} \quad (4.53)$$

Since we do not have the solution of ϕ_2 , the constant term in (4.53) can not be determined. Except for the arbitrary constant A_0 , so far we have the leading order plus the $O(\varepsilon)$ correction of the vertical structure. Moreover we have obtained K_0 , K_1 and K_2 as functions of b , c_0 , c_1 and c_2 . To determine c , we shall turn our attention to the fast variation meridional structure.

From (4.16), Q can be approximated as

$$Q^2 \cong \frac{\mu^2}{1-\mu^2} \left\{ \frac{K_0^2}{\mu^2(1-\mu^2)} - K_0^2 - \varepsilon 2K_0K_1 - \varepsilon^2 (2K_0K_2 + K_1^2) \right\} \quad (4.54)$$

Since K_0 is a constant, the leading order of (4.54) is the same as (3.10). From (4.17) and (4.18), the leading order asymptotic solution for χ is

$$\chi \sim (Q^2)^{-1/4} \exp\left\{ \pm \varepsilon^{-2} \int^{\mu} (Q^2)^{1/2} d\mu \right\} \quad (4.55)$$

As discussed in chapter iii, in order that χ has a nontrivial solution, we must have at least one turning point where $Q \leq O(\epsilon^2)$. This requires that K_0 be equal or larger than $2k_0$. For $K_0 > 2k_0$, from the previous chapter, we note that there are two locations where the $O(1)$ term in (4.54) is zero. Since both K_0 and c_1 are constant while b is a function of μ , from (4.42), we know that K_1 can not be zero at both locations. Therefore K_0 can not be larger than $2k_0$. For $K_0 = 2k_0$, the $O(1)$ term in (4.54) has a double root at $\mu = \mu_0$,

$$\frac{k_0^2}{\mu^2(1-\mu^2)} - K_0^2 = 0, \quad \text{at } \mu = \mu_0 = \sqrt{\frac{1}{2}} \quad (4.56)$$

At this location, we can set $2K_0K_1$ to zero by requiring that

$$K_0^2 c_1 = \frac{1}{2} + b_0 e^{-2(-E_1(2) + i\pi)} \quad (4.57)$$

where

$$b_0 = \frac{\beta_s}{\mu_0^2} + 1 = 2\beta_s + 1 \quad (4.58)$$

Therefore $2k_0$ is the only possible value of K_0 . Consequently there is a single location, $\mu_0 = \sin(45^\circ)$, where $Q \leq O(\epsilon^2)$. Since the leading order of Q has a double root at this point, we will refer to this point as a second-order turning point. We note that the value of K_0 is different from that of chapter iii. The main reason is that, since Q is approximated as a perturbation series in (4.54), the difference

between K_0 and $2k_0$ in the previous chapter is present only at $O(\epsilon^2)$ here.

Since Q will not be an $O(1)$ quantity as $\mu \rightarrow \mu_0$, the WKB solution is not valid in this region. We need a local solution of (4.8) to properly describe the behavior of ψ in this region. Therefore we expand coefficients in Taylor series around μ_0 and change variable from μ to y , where

$$y = \epsilon^{-1} (\mu - \mu_0) \quad (4.59)$$

In terms of y , (4.8) becomes

$$\begin{aligned} \frac{\partial^2 \psi}{\partial \zeta^2} - \epsilon \frac{\partial \psi}{\partial \zeta} - (1 + \epsilon^2 8y^2) K_0^2 \psi + \epsilon^2 \frac{\partial^2 \psi}{\partial y^2} \\ + \frac{\epsilon \psi}{\zeta - c_0} (b_0 - \epsilon 4 \sqrt{2} \beta_s y) + O(\epsilon^3) = 0 \end{aligned} \quad (4.60)$$

The upper and lower boundary conditions remain the same as (4.6) and (4.9). As in the WKB regime, near $\zeta = c_0$, we change variable from ζ to $\xi = \epsilon^{-1}(\zeta - c_0)$. The resulting equation for this inner region is

$$\frac{\partial^2 \psi^i}{\partial \xi^2} - \epsilon^2 \frac{\partial \psi^i}{\partial \xi} - \epsilon^2 K_0^2 \psi^i + \frac{\epsilon^2 b_0 \psi^i}{\xi - c_1 - \epsilon c_2 - \dots} + O(\epsilon^3) = 0 \quad (4.61)$$

The first three order perturbation equations for ψ are

$$\frac{\partial^2 \psi_0}{\partial \zeta^2} - K_0^2 \psi_0 = L_0 \psi_0 = 0 \quad (4.62)$$

$$L_0 \psi_1 = \frac{\partial \psi_0}{\partial \zeta} - \frac{b_0 \psi_0}{\zeta - c_0} \quad (4.63)$$

and

$$L_0 \psi_2 = \frac{\partial \psi_1}{\partial \zeta} - \frac{b_0 \psi_1}{\zeta - c_0} - \frac{\partial^2 \psi_0}{\partial y^2} + 8K_0^2 y^2 \psi_0 + \frac{4\sqrt{2} \beta_s \psi_0}{\zeta - c_0} - \frac{c_1 b_0 \psi_0}{(\zeta - c_0)^2} \quad (4.64)$$

As for ψ^i , the first three order perturbation equations are

$$\frac{\partial^2 \psi_0^i}{\partial \xi^2} = 0 = L_0^i \psi_0^i \quad (4.65)$$

$$L_0^i \psi_1^i = 0 \quad (4.66)$$

and

$$L_0^i \psi_2^i = \frac{\partial \psi_0^i}{\partial \xi} + K_0^2 \psi_0^i - \frac{b_0 \psi_0^i}{\xi - c_1} \quad (4.67)$$

Since the leading order equation and boundary conditions for ψ are the same as those in the WKB regime, the solution is the same as (4.31) except now the coefficient may be a function of y , i.e.,

$$\psi_0 = B_0(y) e^{-K_0(\zeta - c_0)} \quad (4.68)$$

The lower boundary condition gives the same condition as (4.32).
Now K_0 is a known value, we can determine c_0 ,

$$c_0 = \frac{1}{K_0} = \frac{1}{2k_0} \quad (4.69)$$

We note that c_0 is real and is inversely proportional to the zonal wavenumber only. This is different from the result of Branscome(1983) where c_0 is inversely proportional to the total wavenumber. After matching with (4.68), the leading order inner solution ψ^i is

$$\psi_0^i = B_0(y) \quad (4.70)$$

The procedure to solve (4.63) and (4.66) is the same as that for the WKB regime. The solutions for them are,

$$\psi_1 = B_0 e^{-K_0(\zeta-c_0)} \left\{ \frac{\zeta}{2} + \frac{b_0}{2K_0} \left[e^{2K_0(\zeta-c_0)} E_1(2K_0(\zeta-c_0)) + \ln K_0(\zeta-c_0) \right] \right\} \quad (4.71)$$

and

$$\psi_1^j = B_0 \left\{ -K_0 \xi + \frac{1}{2K_0} [1 - b_0(E_0 + \ln 2)] \right\} \quad (4.72)$$

The lower boundary condition for ψ_1 gives the same result as (4.58), therefore c_1 can be written as

$$c_1 = \frac{1}{K_0^2} \left\{ \frac{1}{2} - b_0 e^{-2} (E_1(2) - i\pi) \right\} \quad (4.73)$$

We note that, due to the existence of the basic state potential vorticity gradient, c_1 is complex. Therefore the leading order growth rate will depend on the magnitude of β_s . Furthermore, since K_0 is inversely proportional to the zonal wavenumber, both c_1 and ψ_1 will become large as the wave becomes longer. Hence these perturbation expansions will break down for long waves.

After matching with ψ_0 and ψ_1 , the second order inner solution is

$$\begin{aligned} \psi_2^i = B_0 \left\{ \frac{K_0^2 \xi^2}{2} - b_0 (\xi - c_1) \ln K_0 (\xi - c_1) \right. \\ \left. + \frac{b_0 \xi}{2} (2 - E_0 - \ln 2) \right\} + \text{constant} \end{aligned} \quad (4.74)$$

As in the WKB region, we will not solve (4.64). Instead, we require that the solvability condition for ψ_2 be satisfied. This yields that

$$\begin{aligned} \frac{\partial^2 B_0}{\partial y^2} - B_0 \left\{ 8K_0^2 y^2 + 8\sqrt{2} K_0 \beta_s e^{-2} E_1(-2) + \frac{1}{4} - \frac{b_0}{2} (e^{-2} E_1(-2) - i\pi) \right. \\ \left. + 2K_0^3 c_2 - b_0^2 e^{-2} F + K_0^2 c_1 b_0 (2 + 3e^{-2} E_1(-2) - i\pi) - K_0^2 c_1 \right\} = 0 \end{aligned} \quad (4.75)$$

where the definition of F is the same as (4.52). We change variable from y to Y where

$$Y = (32K_0^2)^{1/4} \left(y + \frac{\beta_s e^{-2} E_1(-2)}{\sqrt{2} K_0} \right) = \varepsilon^{-1} (32K_0^2)^{1/4} \left(\mu - \mu_0 - \frac{\varepsilon \beta_s e^{-2} (E_1(2) - i\pi)}{\sqrt{2} K_0} \right) \quad (4.76)$$

In terms of Y , (4.75) becomes a parabolic cylinder equation,

$$\frac{\partial^2 B_0}{\partial Y^2} + \left(\nu + \frac{1}{2} - \frac{Y^2}{4} \right) B_0 = 0 \quad (4.77)$$

where we define that

$$\begin{aligned} \nu + \frac{1}{2} = \frac{1}{(32K_0^2)^{1/4}} \{ & b_0^2 e^{-2} F - 2K_0^3 c_2 + \frac{1}{4} - b_0 + (2\beta_s e^{-2} E_1(-2))^2 \\ & - b_0^2 e^{-2} E_1(-2) (3e^{-2} E_1(-2) + 2 - i\pi) \} \end{aligned} \quad (4.78)$$

Since the meridional boundary conditions require that χ be zero at both boundaries, the leading order asymptotic solutions of χ away from the turning point are

$$\chi \sim D_1(Q^2)^{-1/4} \exp\left\{ -\varepsilon^{-2} \int_{\mu_0}^{\mu} (Q^2)^{1/2} d\tau \right\}, \quad \text{for } \mu_0 + O(\varepsilon) < \mu \leq 1 \quad (4.79)$$

$$\chi \sim D_2(Q^2)^{-1/4} \exp\left\{ \varepsilon^{-2} \int_{\mu_0}^{\mu} (Q^2)^{1/2} d\tau \right\}, \quad \text{for } 0 \leq \mu < \mu_0 - O(\varepsilon)$$

(4.80)

The possible solutions for B_0 that can match asymptotically with (4.79) and (4.80) is the parabolic cylinder functions of integer order. Therefore, ν must be an integer. For given $\nu=n$, the solution for B_0 is

$$B_0 = \text{He}_n(Y) e^{-Y^2/4}$$

(4.81)

where He_n is a Hermit polynomials of order n and

$$\text{He}_0(Y) = 1, \quad \text{He}_1(Y) = Y \quad \text{and} \quad \text{He}_2(Y) = Y^2 - 1$$

(4.82)

We note that n is equivalent to the meridional wavenumber. From (4.78), c_2 can be written as

$$c_2 = \frac{1}{2K_0^3} \left\{ -\left(n + \frac{1}{2}\right)(32K_0^2)^{1/2} + b_0^2 e^{-2} F + (2\beta_s e^{-2} E_1(-2))^2 + \frac{1}{4} - b_0 \right. \\ \left. - b_0^2 e^{-2} E_1(-2) (3e^{-2} E_1(-2) + 2 - i\pi) \right\}$$

(4.83)

It is easy to see that c_2 depends on n . Since the perturbation expansion of Q prevents K_0 from being larger than $2k_0$, the meridional wavenumber can not be included in k_0 . Therefore, unlike the solutions in the previous chapter and in β -plane analyses, the contribution from the meridional wavenumber only occurs at $O(\varepsilon^2)$.

Furthermore only the real part of c_2 depends on n , therefore only the phase speed will be a function of the meridional wavenumber at this order. We can not determine the relation between the growth rate and the meridional wavenumber at this order. The numerical analyses (Simmons and Hoskins, 1976; Frederiksen, 1978) indicated that the lowest meridional wavenumber has the largest growth rate. Furthermore, Frederiksen found that the differences among different meridional wavenumbers are small for the short waves, which is consistent with the contributions of the meridional wavenumber to the growth rate and phase speed being small in our solutions.

For given n , after matching (4.81) with (4.79) and (4.80), we can determine D_1 and D_2 . Then the solution of the leading order perturbation streamfunction is complete. In the following, we shall present and discuss some of the results from the above analytic solutions. Since we can not determine the growth rate as a function of the meridional wavenumber, we shall only consider the case $n=1$.

(a). The growth rate and Phase speed

From the above analytic solutions, we note that the growth rate and phase speed are determined at the turning point. For this particular basic flow, the turning point is located at 45° latitude. To $O(\epsilon)$, the dimensional phase speed is

$$\begin{aligned} c_r^* &\equiv \epsilon \frac{U_0}{a} \{ c_0 + \epsilon c_{1r} \} \\ &= \frac{U_0(1-\mu_0^2)^{1/2}}{k} \frac{f_0}{N_0 H} \left\{ 1 + \frac{a(1-\mu_0^2)^{1/2}}{k} \frac{f_0}{N_0 H} \left(\frac{1}{2} - 0.67 \left(1 + \frac{\beta_s}{\mu_0^2} \right) \right) \right\} \end{aligned} \quad (4.84)$$

where

$$f_0 = 2\Omega\mu_0 \quad \text{and} \quad \mu_0 = \sqrt{\frac{1}{2}}$$

f_0 is the Coriolis parameter at the turning point. We note that

$$\frac{\beta_s}{\mu_0^2} = \frac{N_0^2 H^2}{2\Omega a U_0 \mu_0^2} = \frac{\beta_0 N_0^2 H^2}{f_0^2 U_0 (1-\mu_0^2)^{1/2}} \quad (4.85)$$

and

$$\beta_0 = \frac{2\Omega(1-\mu_0^2)^{1/2}}{a} \quad (4.86)$$

is the gradient of the Coriolis parameter. Since $U_0(1-\mu_0^2)^{1/2}$ is the velocity of the basic flow at 45° , (4.85) is the same as the γ parameter of Branscome(1983), which is

$$\gamma = \frac{\beta_0 N_0^2 H}{f_0^2 \frac{\partial U}{\partial z}} \quad (4.87)$$

In fact, if $a(1-\mu_0^2)^{1/2}/k$ is replaced by the total wavenumber on a β -plane, then (4.84) is identical to that of Branscome's study. Since β_s is positive for westerly flow, the $O(\epsilon)$ correction of the phase speed is always negative and is larger for longer waves.

To $O(\epsilon^2)$, in terms of γ , the dimensional growth rate is

$$\begin{aligned} \sigma_i &= \epsilon k \frac{U}{a} (\epsilon c_{1i} + \epsilon^2 c_{2i}) \\ &= 0.425(1+\gamma) \frac{U_0 a(1-\mu_0^2)}{k} \frac{f_0^2}{N_0^2 H^2} \left\{ 1 - \frac{a(1-\mu_0^2)^{1/2}}{k} \frac{f_0}{N_0 H} \left[0.26(1+\gamma) + \frac{0.67\gamma}{1+\gamma} \right] \right\} \end{aligned} \quad (4.88)$$

The maximum growth rate occurs at

$$k_m = 2a(1-\mu_0^2)^{1/2} \frac{f_0}{N_0 H} \left\{ 0.26(1+\gamma) + \frac{0.67\gamma}{1+\gamma} \right\} \quad (4.89)$$

Since k is an integer, the most unstable wavenumber should take the integer value of (4.89). The last term in (4.88) comes from transforming (4.75) into a parabolic cylinder equation. Except for that term, (4.88) and (4.89) are very similar to Branscome's result. Since γ is positive, the $O(\epsilon^2)$ correction to the growth rate is negative. We note that the valid ranges for these perturbation expansions not only depend on the zonal wavenumber but also on the values of the basic state parameters.

Figs. 4.1 and 4.2 show the perturbation's growth rates and phase speeds as functions of the zonal wavenumber k for $U_0=20, 30, 40$ m/sec. and $N_0^2=2 \times 10^{-4}$ sec.⁻². Other basic state parameters are the same as those in chapter iii. Since the growth rate and phase speed are inversely proportional to k , longer waves have larger growth rates and phase speeds. Nonetheless, as k becomes smaller, the corrections to the growth rate and phase speed become larger, these growth rates and phase speeds will become negative for long waves. Therefore these perturbation expansions are not valid for long waves. Since the growth rate and phase speed are proportional to U_0 , larger U_0 have larger growth rates and phase speeds. The differences among the growth rates and the phase speeds of different values of U_0 are larger for longer waves. Furthermore, the maximum growth rate and phase speed shift toward longer waves as U_0 becomes larger. These maxima occur at the wavenumbers near the limit of the shortwave expansion.

Figs. 4.3 and 4.4 are the same as those in figs. 4.1 and 4.2, except for $N_0^2 = 1 \times 10^{-4}$, 2×10^{-4} , 3×10^{-4} sec^{-2} and $U_0 = 30$ m/sec. As

expected, the growth rate and phase speed are inversely proportional to the static stability. The maximum growth rate shifts toward longer waves as N_0 becomes smaller, but the maximum phase speed shifts toward shorter waves as N_0 becomes smaller.

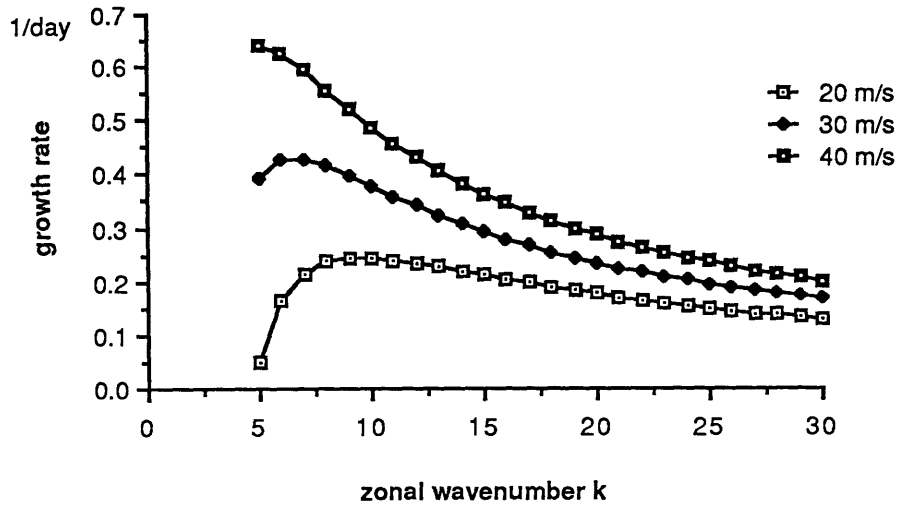


Fig. 4.1. The perturbation's growth rates for solid body rotation as functions of the zonal wavenumber k for $U_0 = 20, 30, 40$ m/sec., $N_0^2 = 2 \times 10^{-4} \text{ sec.}^{-2}$ and other basic state parameters the same as chapter iii.

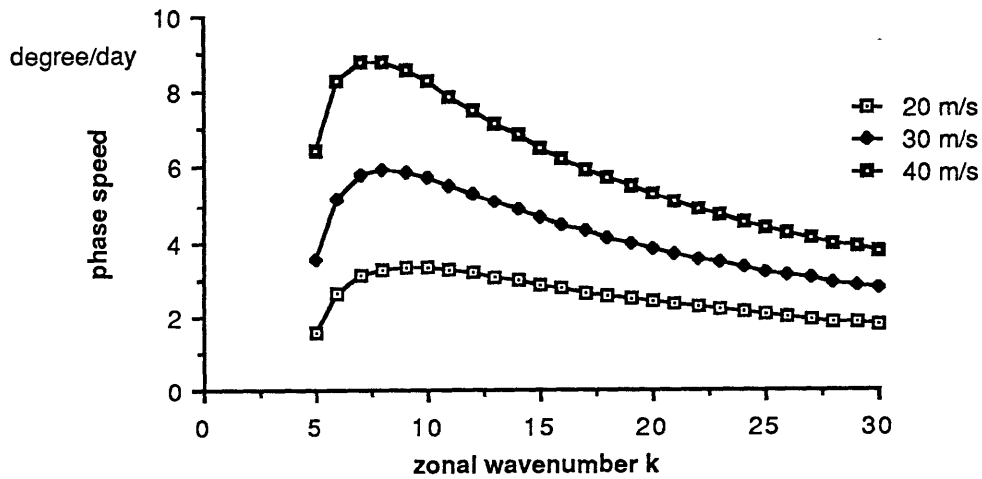


Fig. 4.2. As in Fig. 4.1, except for the phase speeds.

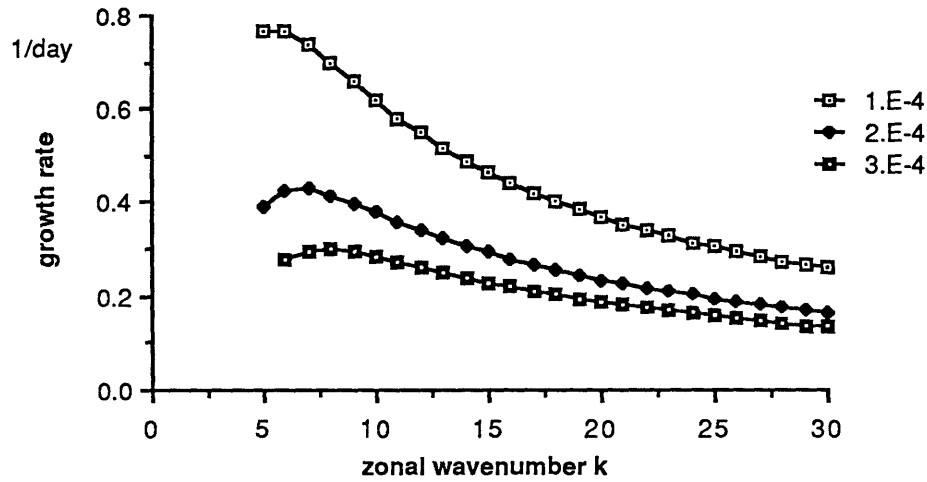


Fig. 4.3. The growth rates as functions of the zonal wavenumber k for $N_0^2 = 1 \times 10^{-4}$, 2×10^{-4} , 3×10^{-4} sec^{-2} ., $U_0 = 30$ m sec^{-1} and other basic state parameters the same as those in chapter iii.

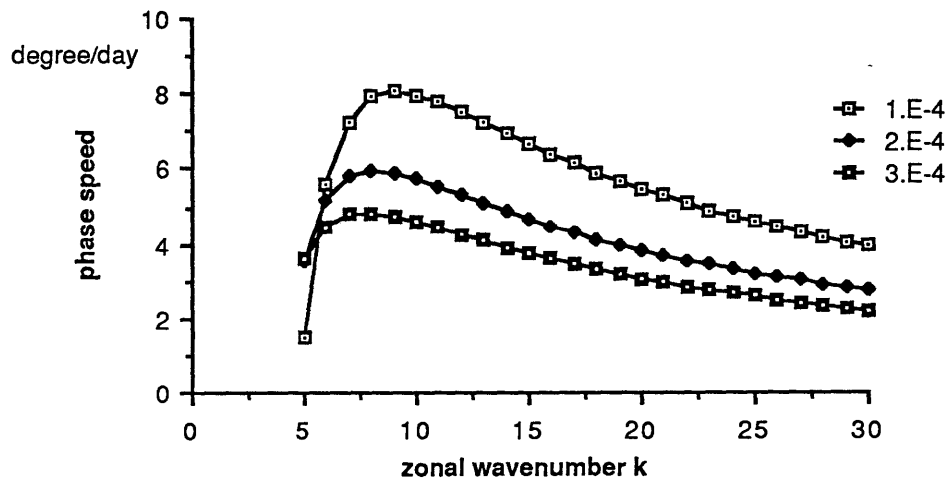


Fig. 4.4. As in Fig. 4.3, except for the phase speeds.

(b). The meridional structure of the unstable wave

Since χ exponentially decays toward both the equator and pole, the primary meridional structure is near the turning point. From (4.76) and (4.81), we note that B_0 decays and oscillates with a meridional scale of ε^{-1} . Since k is scaled by ε^{-2} , the perturbation's meridional scale should be proportion to the order of $k^{1/2}$. Furthermore B_0 has a maximum at $\text{Re}(Y)=0$, therefore the perturbation's maximum amplitude is located at,

$$\mu_m = \mu_0 + \frac{\varepsilon \beta_s e^{-2} E_1(2)}{\sqrt{2} K_0} \quad (4.90)$$

Figs. 4.5 and 4.6 show μ_m as a function of k for different values of U_0 and N_0 . Since the $O(\varepsilon)$ correction to μ_m is positive, it is located on the poleward side of the turning point. This poleward deviation from μ_0 is inversely proportional to the zonal wavenumber k , so μ_m moves away from μ_0 as the wave becomes longer and approaches μ_0 as the wave becomes shorter. Furthermore, this deviation from μ_0 is proportional to U_0 and is inversely proportional to N_0 . Figs. 4.7 and 4.8 show the leading order of the meridional amplitude and phase variation as functions of latitude for $k=8,16,24$ and $n=1$. We note that the amplitudes decay rapidly away from μ_m . The meridional scale decreases as the zonal scale decreases, but the phase does not differ much for different k . Furthermore, the existence of the

meridional phase variation implies that an eddy momentum flux is present in this problem.

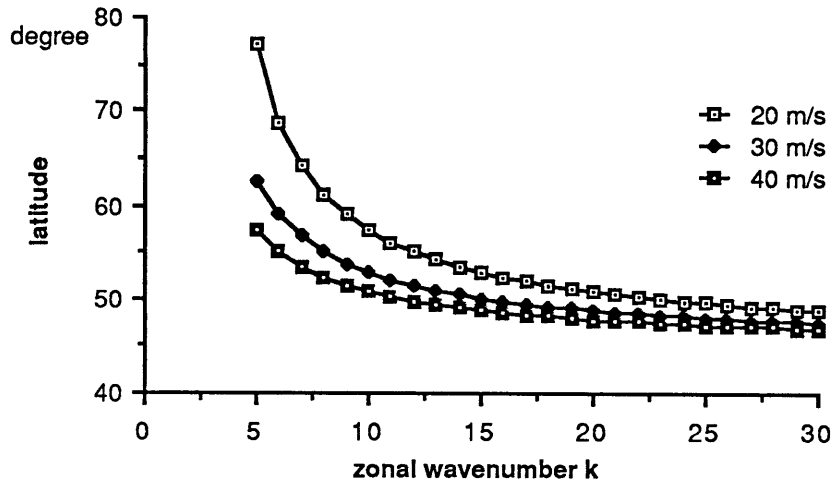


Fig. 4.5 The location of the perturbation's maximum amplitude as a function of the zonal wavenumber k for $U_0=20, 30$ and 40 m/sec..

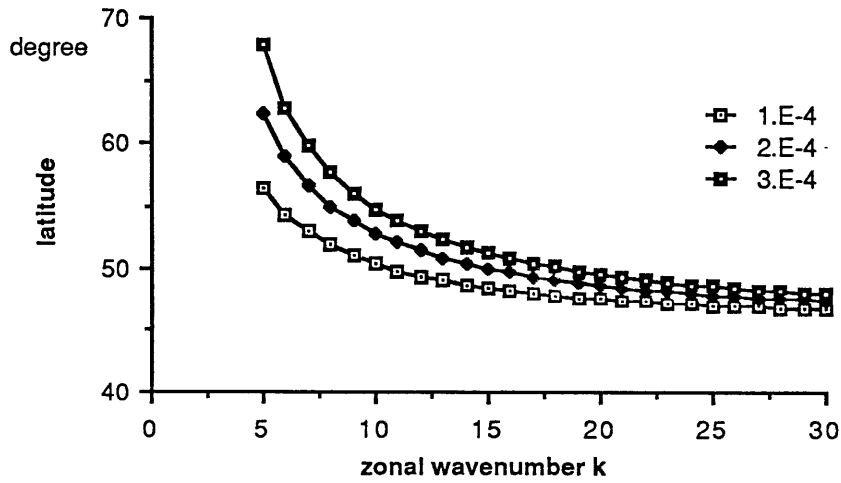


Fig. 4.6. As in Fig. 4.5, except for: $N_0^2 = 1 \times 10^{-4}, 2 \times 10^{-4}, 3 \times 10^{-4}$ sec⁻².

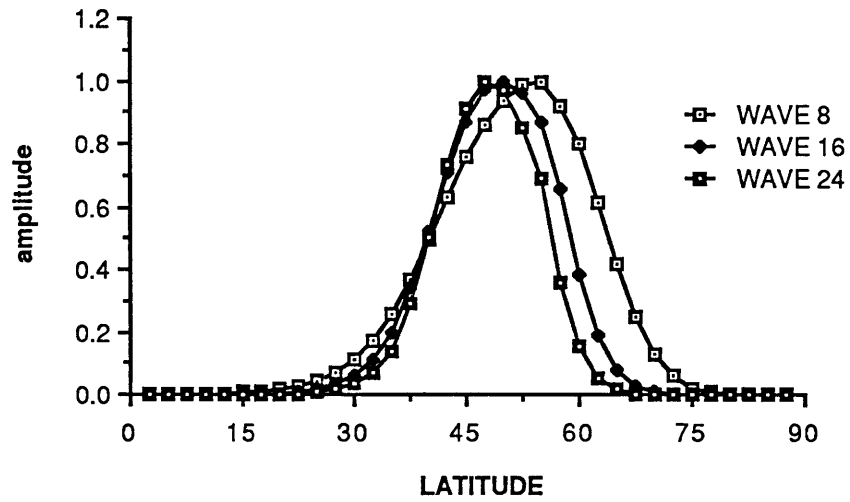


Fig. 4.7. The meridional amplitude functions of $k=8, 16, 24$ and $n=1$ for $U_0=30$ m/sec. and $N_0^2=2 \times 10^{-4}$ sec.⁻².

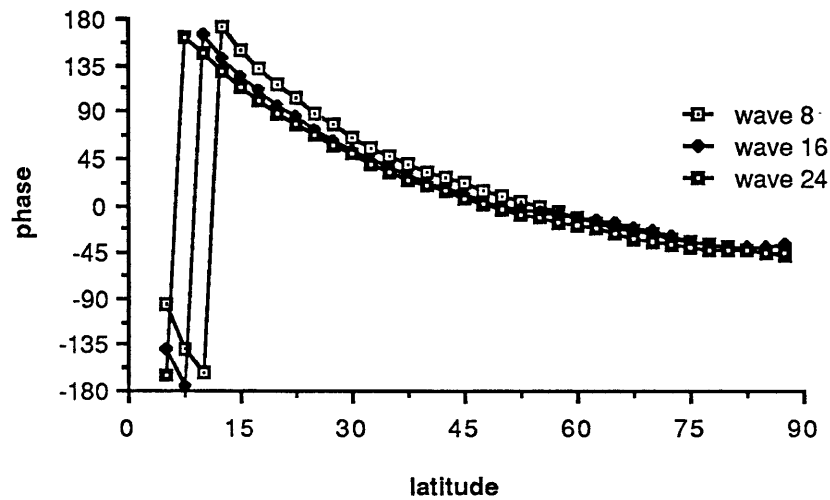


Fig. 4.8. As in Fig. 4.7, except for the meridional phase variation.

(c). The vertical structure of the unstable wave

From (4.31) and (4.68), we note that the perturbation's leading order vertical structure is an exponentially decreasing function of height. Since K_0 is a constant and $K_0=2k_0$, the vertical scale is proportional to the zonal scale and does not vary with latitude. Due to the existence of the basic state potential vorticity gradient, the $O(\epsilon)$ correction to ϕ is complex. Therefore there is an $O(\epsilon)$ phase variation with height.

Fig. 4.9 shows, to $O(\epsilon)$, the perturbation's vertical amplitudes at the turning point as functions of height for the zonal wavenumbers 8, 16 and 24. Since the meridional variation of the vertical structure only exists at $O(\epsilon)$, the amplitude profiles at other latitudes may not differ too much from these profiles at the turning point. We note that longer waves have deeper scales. Since, from (4.67), ψ_1 is inversely proportional to K_0 , the $O(\epsilon)$ correction to the vertical structure will be larger for longer waves. Therefore, as shown in fig. 4.9, the lowest wavenumber has a more complex structure. The maximum amplitudes occur at the surface. Fig. 4.10 shows the leading order phases of the vertical structures. We note that the magnitude of the phases decrease with height, which implies the phases of these unstable waves tilt upward and westward. As mentioned in chapter iii, this is the condition for the conversion of the available potential energy of the basic flow to the growth of the perturbation. Furthermore, the magnitude and scale of the phase change decrease as the zonal wavenumber increases.

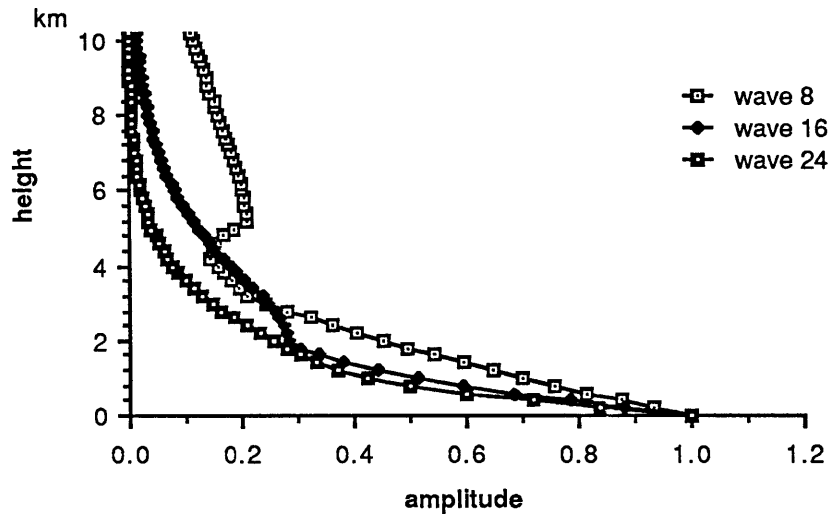


Fig. 4.9. As in Fig. 4.7, except for the amplitudes as functions of height at the turning point, which is located at 45° latitude.

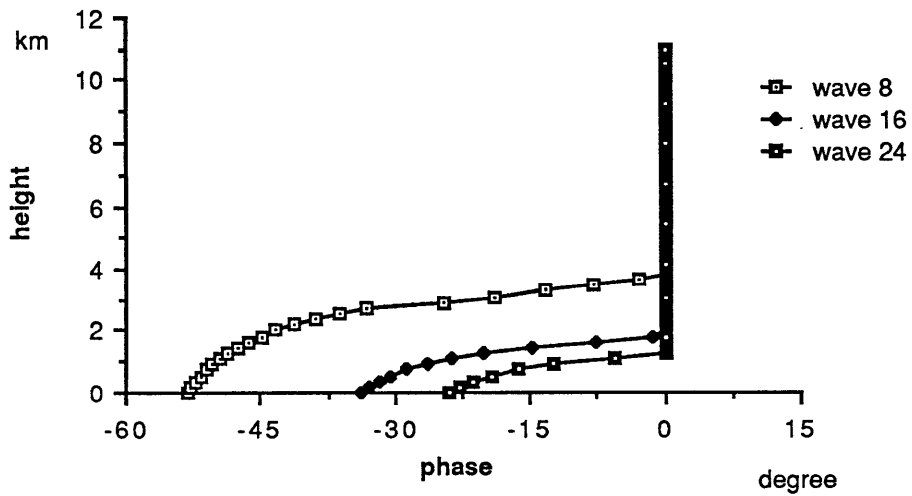


Fig. 4.10. As in Fig. 4.9, except for the vertical phase variations.

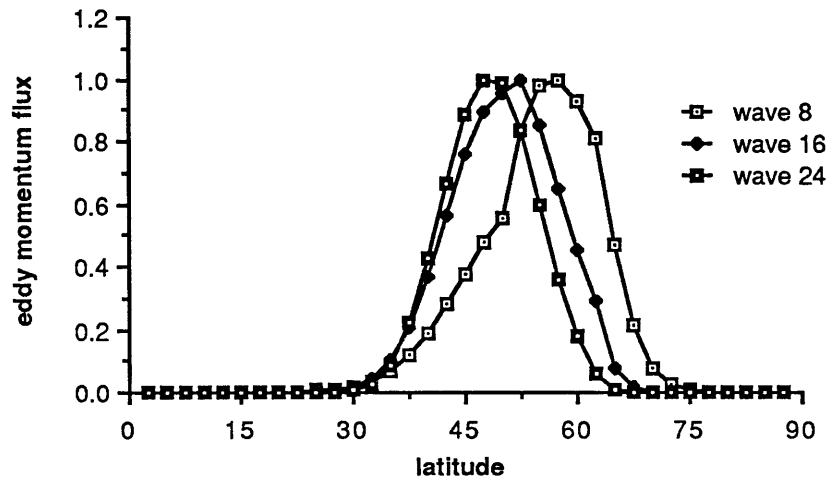


Fig. 4.11. As in Fig. 4.7, except for the eddy momentum fluxes.

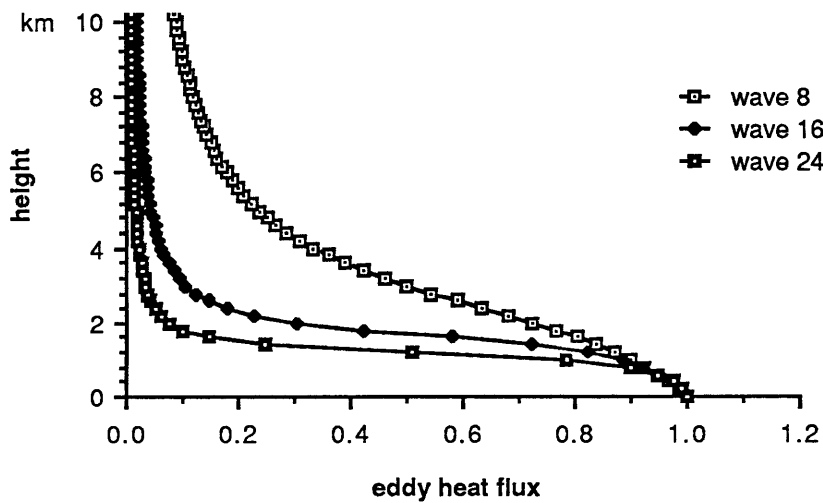


Fig. 4.12. As in Fig. 4.9, except for the eddy heat fluxes at the turning point.

(d). The eddy fluxes

The eddy momentum and heat fluxes can be written as,

$$\overline{vT} = \frac{1}{(1-\mu^2)^{1/2}} \overline{\frac{\partial \Psi}{\partial \lambda} \frac{\partial \Psi}{\partial z}} = \frac{ke^{2kc_1 t}}{2(1-\mu^2)^{3/2}} |\phi|^2 |\chi|^2 \epsilon^{-1} \frac{\partial \alpha_v}{\partial \zeta} \quad (4.91)$$

and

$$\overline{uv} = \overline{\frac{\partial \Psi}{\partial \lambda} \frac{\partial \Psi}{\partial \mu}} = -\frac{ke^{2kc_1 t}}{2(1-\mu^2)} |\phi|^2 |\chi|^2 \frac{\partial \alpha_\mu}{\partial \mu} \quad (4.92)$$

where α_v is the vertical phase and α_μ is the meridional phase.

Because of the presence of the basic state potential vorticity gradient, the unstable perturbations in this model not only have vertical phase variations but also have meridional phase variations. Therefore both fluxes are nonzero in this model.

Fig. 4.11 shows the eddy momentum fluxes as functions of latitude for the zonal wavenumbers 8, 16 and 24. We note that, since the momentum flux is proportional to $|\chi|^2$, these profiles are similar to the amplitude profiles, but with smaller meridional scales. From (4.92), we note that the eddy momentum flux is proportional to the gradient of the perturbation's meridional phase. Since the gradient of these phases, as shown in fig. 4.8, do not change sign, these momentum fluxes are poleward everywhere. Fig. 4.12 shows the eddy heat fluxes as functions of height at the turning point. We note that, near the surface, the eddy heat fluxes do not decrease as

rapidly as the amplitudes of the perturbations. But the magnitude of these fluxes decreases very rapidly near the critical layer.

From the above discussion, we note that this particular problem on the sphere is very closely related to the baroclinic instability problem on a β -plane. The perturbation's growth rate, phase speed and the vertical structure are almost identical to those from Branscome(1983). Nonetheless the spherical geometry plays an important role in determining the location of the maximum amplitude and the eddy momentum flux. Although these analytic solutions are not valid at long waves, they provide simple analytic expressions for the perturbation's growth rate, phase speed, vertical structure and meridional structure. Moreover we have learned how and where the growth rate and phase speed were determined.

The above analytic procedure, which consists of a two-scale formalism and a local expansion method, is more elaborate than those used heretofore in the β -plane analyses where only one of these two methods was adopted. The application of the local expansion near the turning point showed that only one turning point can exist in our solutions. Thus the perturbation's meridional structure near the turning point can only be approximated by a parabolic cylinder function of integer order. The existence of a second-order turning point is not an essential difference between our solutions and those on the β -plane with two first order turning points(Ioannou and Lindzen, 1986). In fact, our second-order

turning point is a limiting case of the two first order turning points problem. We note that the connection condition for the two-turning-point problem is

$$\int_{\mu_1}^{\mu_2} (-Q^2)^{1/2} d\mu = \varepsilon^2 \left(n + \frac{1}{2} \right) \pi$$

$$\cong \overline{(-Q^2)^{1/2}} (\mu_2 - \mu_1)$$

where μ_1, μ_2 are the first order turning points. This is just Ioannou and Lindzen's Eq. (2.12) written in our notation. When ε is small, these turning points must be very close to each other, i.e., close compared to the radius of deformation. In the asymptotic limit, we can combine these two turning points into a single second-order turning point and approximate the solution in this region by a parabolic cylinder function of integer order. Note however that the width of the region which joins together the exponentially decaying solutions is of order the square root of the zonal wavenumber both in our solutions (see Eqs. 4.76 and 4.56) and in the β -plane solutions (Ioannou and Lindzen, 1986). Because of our shortwave approximation, this width is of order the radius of deformation in our solutions.

From the above solutions, we note that the vertical structure in the WKB regime when evaluated at the turning point is the same as that in the turning point solution, and the leading order meridional structure can be directly derived from (4.12) by requiring that it be

approximated by a parabolic cylinder function of integer order near the turning point. Therefore, to determine the properties of the unstable baroclinic waves, we only need to solve the perturbation equations in the WKB regime. In the following chapter, we will adopt this simplified procedure to study the instability properties of a general meridional profile.

CHAPTER V

A GENERAL MERIDIONAL PROFILE PROBLEM

Since the procedure developed in the last chapter is not limited to finding analytic solutions for that particular problem, we can apply it to investigate the instability problem of a general meridional profile. By comparing with numerical calculations (Simmons and Hoskins, 1976), we can also determine if our analytic solutions give reasonable results. Moreover, from these analytic solutions, we shall be able to find out how and where the properties of baroclinic unstable waves on the sphere are determined.

In this chapter, we assume that the basic flow is

$$\bar{u} = M(\mu) z \tag{ 5.1 }$$

where M is the unspecified meridional structure and the vertical structure is still taken as a linear function of height. Other basic state parameters are the same as those in the last chapter. By assuming that the perturbation streamfunction has a normal mode solution as that in (4.2), the governing equation for this general profile can be written as

$$\begin{aligned}
& \frac{\partial^2 \psi}{\partial z^2} - \frac{\partial \psi}{\partial z} - \varepsilon^2 \frac{k^2 - 1}{\mu^2(1-\mu^2)} \psi + \varepsilon^2 \frac{1-\mu^2}{\mu^2} \frac{\partial^2 \psi}{\partial \mu^2} + \frac{\psi}{z - \frac{(1-\mu^2)^{1/2}}{c} M} \left\{ 1 \right. \\
& \quad \left. + \frac{\beta_s (1-\mu^2)^{1/2}}{\mu^2 M} - \frac{\varepsilon^2 (1-\mu^2)^{1/2} z}{\mu^2 M} \frac{\partial^2}{\partial \mu^2} [(1-\mu^2)^{1/2} M] \right\} = 0
\end{aligned}
\tag{5.2}$$

We see that M appears only in those terms that are associated with the basic state potential vorticity gradient. The boundary conditions for ψ are

$$c \frac{(1-\mu^2)^{1/2}}{M} \frac{\partial \psi}{\partial z} + \psi = 0, \quad \text{at } z = 0 \tag{5.3}$$

and

$$\psi = 0 \quad \text{as } z \rightarrow \infty \quad \text{and at } \mu = 0, 1 \tag{5.4}$$

Since c is multiplied by $(1-\mu^2)^{1/2}/M$, except for a solid body rotation, the lower boundary condition will no longer be independent of latitude. This dependence on μ may cause the perturbation's leading order vertical structure to vary with latitude.

As in the last chapter, we adopt the shortwave approximation and change variables from z to ζ . After rescaling, (5.2) becomes

$$\begin{aligned}
\frac{\partial^2 \psi}{\partial \zeta^2} - \varepsilon \frac{\partial \psi}{\partial \zeta} - \frac{k_0^2 - \varepsilon^4}{\mu^2(1-\mu^2)} \psi + \varepsilon^4 \frac{1-\mu^2}{\mu^2} \frac{\partial^2 \psi}{\partial \mu^2} + \frac{\varepsilon \psi}{\zeta - \frac{(1-\mu^2)^{1/2}}{M} c} \left\{ 1 \right. \\
\left. + \frac{\beta_s (1-\mu^2)^{1/2}}{\mu^2 M} - \frac{\varepsilon^3 (1-\mu^2)^{1/2} \zeta}{\mu^2 M} \frac{\partial^2}{\partial \mu^2} [(1-\mu^2)^{1/2} M] \right\} = 0
\end{aligned} \tag{5.5}$$

where k_0 , c and ζ are the same as (4.7). To separate the perturbation's fast variation meridional structure from the vertical structure, we assume that

$$\psi = \phi(\mu, \zeta) \chi(\eta) \tag{5.6}$$

where η is the fast variation meridional variable and is the same as (4.11). The governing equation for χ is again of the form

$$\frac{\partial^2 \chi}{\partial \eta^2} - Q^2 \chi = \varepsilon^4 \frac{\partial^2 \chi}{\partial \mu^2} - Q^2 \chi = 0 \tag{5.7}$$

After substituting (5.6) and (5.7) into (5.5), the governing equation for ϕ is

$$\begin{aligned}
\frac{\partial^2 \phi}{\partial \zeta^2} - \varepsilon \frac{\partial \phi}{\partial \zeta} - K^2 \phi + \frac{\varepsilon^4 \phi}{\mu^2(1-\mu^2)} + \varepsilon^2 \frac{1-\mu^2}{\mu^2} \left\{ \frac{2 \partial \chi}{\chi} \frac{\partial \phi}{\partial \eta} \frac{\partial \phi}{\partial \mu} + \varepsilon^2 \frac{\partial^2 \phi}{\partial \mu^2} \right\} \\
+ \frac{\varepsilon \phi}{\zeta - \frac{(1-\mu^2)^{1/2}}{M} c} \left\{ b - \frac{\varepsilon^3 (1-\mu^2)^{1/2} \zeta}{\mu^2 M} \frac{\partial^2}{\partial \mu^2} [(1-\mu^2)^{1/2} M] \right\} = 0
\end{aligned} \tag{5.8}$$

where we define that

$$b = \frac{\beta_s (1-\mu^2)^{1/2}}{\mu^2 M} + 1 \quad (5.9)$$

$$K^2 = \frac{k_0^2}{\mu^2(1-\mu^2)} - \frac{1-\mu^2}{\mu^2} Q^2 \quad (5.10)$$

b is the leading order of the basic state potential vorticity gradient and is a function of μ and M . K is a function of zonal wavenumber and Q . As mentioned in the last chapter,

$$\frac{1}{\chi} \frac{\partial \chi}{\partial \eta} = \sum_{n=0}^{\infty} \varepsilon^{2n} q_n, \quad (5.11)$$

therefore (5.8) does not depend on χ or η . The boundary conditions for ϕ and χ are

$$\frac{(1-\mu^2)^{1/2}}{M} c \frac{\partial \phi}{\partial \zeta} + \phi = 0, \quad \text{at } \zeta = 0 \quad (5.12)$$

$$\phi = 0, \quad \text{as } \zeta \rightarrow \infty \quad (5.13)$$

and

$$\chi = 0, \quad \text{at } \mu = 0, 1 \quad (5.14)$$

Now we can apply the perturbation method to solve (5.8). The perturbation expansions of ϕ , K and c are the same as those of (4.24). The first three order perturbation equations for ϕ are

$$\frac{\partial^2 \phi_0}{\partial \zeta^2} - K_0^2 \phi_0 = L_0 \phi_0 = 0 \quad (5.15)$$

$$L_0 \phi_1 = \frac{\partial \phi_0}{\partial \zeta} + 2K_0 K_1 \phi_0 - \frac{b \phi_0}{\zeta - \frac{(1-\mu^2)^{1/2}}{M} c_0} = L_1 \phi_0 \quad (5.16)$$

$$L_0 \phi_2 = L_1 \phi_1 + (2K_0 K_2 + K_1^2) \phi_0 - \frac{1-\mu^2}{\mu^2} \frac{2}{\chi} \frac{\partial \chi}{\partial \eta} \frac{\partial \phi_0}{\partial \mu} - \frac{\frac{c_1 (1-\mu^2)^{1/2}}{M} b \phi_0}{\left(\zeta - \frac{(1-\mu^2)^{1/2}}{M} c_0\right)^2} \quad (5.17)$$

The upper boundary condition for ϕ_n is

$$\phi_0 = \phi_1 = \phi_2 = \dots = 0, \quad \text{as } \zeta \rightarrow \infty \quad (5.18)$$

At $\zeta=0$, the condition for ϕ_n is

$$\frac{(1-\mu^2)^{1/2}}{M} c_0 \frac{\partial \phi_0}{\partial \zeta} + \phi_0 = 0 \quad (5.19)$$

$$\frac{(1-\mu^2)^{1/2}}{M} c_0 \frac{\partial \phi_1}{\partial \zeta} + \phi_1 = - \frac{(1-\mu^2)^{1/2}}{M} c_1 \frac{\partial \phi_0}{\partial \zeta} \quad (5.20)$$

$$\frac{(1-\mu^2)^{1/2}}{M} c_0 \frac{\partial \phi_2}{\partial \zeta} + \phi_2 = - \frac{(1-\mu^2)^{1/2}}{M} c_1 \frac{\partial \phi_1}{\partial \zeta} - \frac{(1-\mu^2)^{1/2}}{M} c_2 \frac{\partial \phi_0}{\partial \zeta} \quad (5.21)$$

As in the last chapter, near $\zeta=c_0(1-\mu^2)^{1/2}/M$, we change variable from ζ to ξ where

$$\xi = \varepsilon^{-1} \left(\zeta - \frac{(1-\mu^2)^{1/2}}{M} c_0 \right) \quad (5.22)$$

Since c_0 is multiplied by $(1-\mu^2)/M$, in general, the critical layer will vary with latitude. In terms of ξ , (5.8) becomes

$$\frac{\partial^2 \phi^i}{\partial \xi^2} - \varepsilon^2 \frac{\partial \phi^i}{\partial \xi} - \varepsilon^2 K^2 \phi^i + \frac{\varepsilon^2 b \phi^i}{\xi - \frac{(1-\mu^2)^{1/2}}{M} (c_1 + \varepsilon c_2 + \dots)} + O(\varepsilon^3) = 0 \quad (5.23)$$

The first three perturbation equations for ϕ^i can be written as

$$\frac{\partial^2 \phi_0^i}{\partial \xi^2} = L_0^i \phi_0^i = 0 \quad (5.24)$$

$$L_0^i \phi_1^i = 0 \quad (5.25)$$

$$L_0^i \phi_2^i = \frac{\partial \phi_0^i}{\partial \xi} + K_0^2 \phi_0^i - \frac{b \phi_0^i}{\xi - \frac{(1-\mu^2)^{1/2}}{M} c_1} \quad (5.26)$$

Since the leading order equations for ϕ and ϕ^i are the same as those in the previous chapter, the solutions can readily be written as

$$\phi_0 = A_0(\mu) e^{-(K_0 \zeta - 1)} \quad (5.27)$$

and

$$\phi_0^i = A_0 \quad (5.28)$$

Here, for convenience, we allow A_0 to depend on μ . The lower boundary condition requires that

$$K_0 = \frac{M}{(1-\mu^2)^{1/2} c_0} \quad (5.29)$$

We note that, unless M is a solid body rotation, K_0 is no longer a constant. Therefore, in general, the leading order perturbation's vertical structure will vary with μ and the vertical scale will not remain the same for all latitudes.

From (5.16) and (5.25), the first order solutions for ϕ and ϕ^i are

$$\phi_1 = A_0 e^{-(K_0 \zeta - 1)} \left\{ \left(\frac{1}{2} - K_1 \right) \zeta + \frac{b}{2K_0} \left[e^{2(K_0 \zeta - 1)} E_1 \{ 2(K_0 \zeta - 1) \} + \ln(K_0 \zeta - 1) \right] \right\} \quad (5.30)$$

and

$$\phi_1^i = A_0 \left\{ -K_0 \zeta + \frac{1}{K_0} \left(K_0^2 c_1 \frac{(1-\mu^2)^{1/2}}{M} - b e^{-2} E_1(-2) - \frac{b}{2} (E_0 + \ln 2) \right) \right\} \quad (5.31)$$

where $E_1(x)$ is the same as (4.39) and E_0 is Euler's constant. Since $E_1(x) = -E_1(x) + i\pi$, (5.30) and (5.31) are complex functions below the

critical layer. As discussed in the last chapter, the existence of b is responsible for these complex values in the $O(\epsilon)$ correction.

Substituting (5.30) into (5.20), we have

$$K_1 = \frac{1}{2} + be^{-2}E_1(-2) - K_0^2 c_1 \frac{(1-\mu^2)^{1/2}}{M} \quad (5.32)$$

Since $E_1(-2) = -E_1(2) + i\pi$, K_1 is a complex function. After matching with (5.27) and (5.30), the $O(\epsilon^2)$ inner solution ϕ^i can be written as

$$\begin{aligned} \phi_2^i = A_0 \left\{ \frac{K_0^2 \xi^2}{2} - b \left(\xi - \frac{(1-\mu^2)^{1/2}}{M} c_1 \right) \ln K_0 \left(\xi - \frac{(1-\mu^2)^{1/2}}{M} c_1 \right) \right. \\ \left. + \frac{b\xi}{2} (2 - E_0 - \ln 2) \right\} + \text{constant} \end{aligned} \quad (5.33)$$

In comparison with the solutions of chapter iv, we note that the general profile M makes little change in the form of the solutions. Nonetheless, since K_0 and b implicitly depend on M , the meridional profile of the basic flow may have some effects on the perturbation's vertical structure.

To determine K_2 and A_0 , we just require that the solvability condition for ϕ_2 be met, which gives

$$\begin{aligned}
2K_0K_2 + K_1^2 = & -2K_0^3C_2 \frac{(1-\mu^2)^{1/2}}{M} + b^2e^{-2} \{ F - E_1(-2)[4e^{-2}E_1(-2) + 2 - i\pi] \} \\
& + K_0^2C_1 \frac{(1-\mu^2)^{1/2}}{M} \{ 3K_0^2C_1 \frac{(1-\mu^2)^{1/2}}{M} - 2be^{-2}E_1(-2) - 1 \} \\
& + be^{-2}(1 + e^{-2}E_1(-2)) + \frac{1-\mu^2}{\mu^2} \frac{2}{\chi} \frac{\partial \chi}{\partial \eta} \left\{ \frac{1}{A_0} \frac{\partial A_0}{\partial \mu} - \frac{1}{2K_0} \frac{\partial K_0}{\partial \mu} \right\}
\end{aligned} \tag{5.34}$$

where F is the same as (4.52). Since, in general, K_0 and A_0 are functions of μ , the μ derivative term in (5.17),

$$\frac{1}{\chi} \frac{\partial \chi}{\partial \eta} \frac{\partial \phi_0}{\partial \mu} = A_0 \sum_{n=0}^{\infty} \varepsilon^{2n} q_n \left\{ -\zeta \frac{\partial K_0}{\partial \mu} + \frac{1}{A_0} \frac{\partial A_0}{\partial \mu} \right\} \tag{5.35}$$

will not vanish. Therefore, unlike (4.51), these terms are present in (5.34). Without losing generality, we can eliminate them from K_2 by requiring that

$$A_0 = K_0^{1/2} \tag{5.36}$$

Since K_0 , K_1 and K_2 are known, from (5.10), Q can be approximated as

$$Q^2 \cong \frac{\mu^2}{1-\mu^2} \left\{ \frac{k_0^2}{\mu^2(1-\mu^2)} - K_0^2 - \varepsilon 2K_0K_1 - \varepsilon^2(2K_0K_2 + K_1^2) \right\} \tag{5.37}$$

As discussed in chapter iv, for χ to have a nontrivial solution, we need a second-order turning point within the meridional domain. Furthermore, χ must be approximated by a parabolic cylinder function of integer order. These conditions require that the leading order term of (5.37) and its first derivative be zero at the turning point. Therefore, at $\mu=\mu_0$,

$$\frac{k_0^2}{\mu^2(1-\mu^2)} - K_0^2 = 0 \quad (5.38)$$

and

$$\frac{k_0^2(2\mu^2-1)}{\mu^3(1-\mu^2)^2} - K_0 \frac{\partial K_0}{\partial \mu} = 0 \quad (5.39)$$

Since K_0 depends on c_0 , there are two unknowns, c_0 and μ_0 , in these two equations. Substituting (5.29) and (5.38) into (5.39), we can eliminate k_0 and c_0 and derive an equation for μ_0 ,

$$\frac{\partial M}{\partial \mu} + \frac{M}{\mu} = 0, \quad \text{at } \mu = \mu_0 \quad (5.40)$$

Since, from (2.13),

$$\begin{aligned} \frac{\partial^2 \bar{T}}{\partial \varphi^2} &= -\frac{2\Omega a \rho}{\rho g R} (1-\mu^2)^{1/2} \frac{\partial}{\partial \mu} (\mu M) \\ &= -\frac{2\Omega a \rho}{\rho g R} \mu (1-\mu^2)^{1/2} \left(\frac{\partial M}{\partial \mu} + \frac{M}{\mu} \right) \end{aligned} \quad (5.40a)$$

where φ is latitude, this second-order turning point, μ_0 , is located at the maximum of the meridional temperature gradient. We note that (5.40) depends on M only. Therefore, the location of the turning point is solely determined by the meridional structure of the basic flow. For westerly flow, since the derivative of M must be negative to satisfy (5.40), the turning point is on the poleward side of the maximum of the basic flow. Furthermore, because of the existence of the derivative term in (5.40), the distance between μ_0 and the maximum of the basic flow depends on the meridional scale of the basic flow. If the scale is broader then the distance will be larger and vice versa.

Once the location of the tuning point is determined, c_0 can be found from (5.29) or (5.38), i.e.,

$$c_0 = \frac{M(\mu_0)}{K_0(1-\mu_0^2)^{1/2}} = \frac{\mu_0 M(\mu_0)}{k_0} \quad (5.41)$$

From the local expansion in the last chapter, we note that K_1 must be zero at the turning point to satisfy the lower boundary condition. Therefore, from (5.32), we can determine c_1 as

$$c_1 = \frac{c_0^2(1-\mu_0^2)^{1/2}}{M(\mu_0)} \left\{ \frac{1}{2} + b_0 e^{-2(-E_1(2) + i\pi)} \right\} \quad (5.42)$$

where b_0 is the value of b at $\mu=\mu_0$,

$$b_0 = 1 + \frac{\beta_s (1-\mu_0^2)^{1/2}}{\mu_0^2 M(\mu_0)} \quad (5.43)$$

Away from the turning point, (5.7) has a WKB solution. To satisfy the boundary conditions(5.14), χ must exponentially decay toward both the equator and pole. Therefore the leading order asymptotic solutions for χ are

$$\chi \sim d_1 (Q^2)^{-1/4} \exp\left\{ -\varepsilon^{-2} \int_{\mu_0}^{\mu} (Q^2)^{1/2} d\tau \right\}, \quad \text{for } \mu_0 + O(\varepsilon) < \mu \leq 1 \quad (5.44)$$

$$\chi \sim d_2 (Q^2)^{-1/4} \exp\left\{ \varepsilon^{-2} \int_{\mu_0}^{\mu} (Q^2)^{1/2} d\tau \right\}, \quad \text{for } 0 \leq \mu < \mu_0 - O(\varepsilon) \quad (5.45)$$

Since Q is not an order one quantity near μ_0 , these WKB solutions are not valid in this region. Therefore, we expand Q as a Taylor series around μ_0 ,

$$Q^2 = D_0 (\mu - \mu_0)^2 - \varepsilon D_1 (\mu - \mu_0) - \varepsilon^2 D_2 \quad (5.46)$$

where

$$D_0 = \frac{\partial^2}{\partial \mu^2} \left\{ \frac{k_0^2}{(1-\mu^2)^2} - \mu^2 K_0^2 \right\}_{\mu=\mu_0} \quad (5.47)$$

$$D_1 = \frac{\partial}{\partial \mu} \left(\frac{\mu^2}{1-\mu^2} 2K_0 K_1 \right)_{\mu=\mu_0} \quad (5.48)$$

$$D_2 = \frac{\mu_0^2}{1-\mu_0^2} (2K_0 K_2 + K_1^2)_{\mu=\mu_0} \quad (5.49)$$

Then we change variable from μ to y , where

$$y = \varepsilon^{-1} (4D_0)^{1/4} \left(\mu - \mu_0 - \frac{\varepsilon D_1}{2D_0} \right) \quad (5.50)$$

As discussed in the last chapter, to match with χ in the WKB regime, we need χ be a parabolic cylinder function of integer order in the turning point regime. Therefore, we must require that

$$n + \frac{1}{2} = -(4D_0)^{-1/2} \left(\frac{D_1^2}{4D_0} - D_2 \right) \quad (5.51)$$

here $n=0,1,2,\dots$, is an integer. In terms of y , (5.7) can be approximated as

$$\frac{\partial^2 \chi}{\partial y^2} + \left(n + \frac{1}{2} - \frac{y^2}{4} \right) \chi = 0 \quad (5.52)$$

Its solution is a parabolic cylinder function of order n ,

$$\chi = \text{He}_n(y) \exp\left\{-\frac{y^2}{4}\right\} \quad (5.53)$$

where $\text{He}_n(y)$, as in (4.82), is a Hermit polynomials of order n . As noted in the last chapter, n can be thought of as the meridional wavenumber. For a given n , we can match (5.53) with (5.44) and (5.45) to determine d_1 and d_2 . From (5.34) and (5.49), we can find c_2 as

$$c_2 = \frac{c_0^3(1-\mu_0^2)}{2M^2(\mu_0)} \left\{ \frac{1-\mu_0^2}{\mu_0^2} \left[-(4D_0)^{1/2} \left(n + \frac{1}{2} \right) + \frac{D_1^2}{4D_0} \right] + \frac{1}{4} - b_0 + b_0^2 e^{-2} F \right. \\ \left. - b_0^2 e^{-2} E_1(-2) (3e^{-2} E_1(-2) + 2 - i\pi) \right\} \quad (5.54)$$

We note that only the phase speed is affected by the meridional wavenumber; therefore the growth rate as a function of n can not be determined at this order. To this stage, we have completed the solutions for the perturbation's leading order vertical structure and fast variation meridional structure. Also, we have determined c to $O(\varepsilon^2)$. In the following we shall discuss the properties of these solutions. As in chapter iv, we only consider the case $n=1$.

To compare with the results from Simmons and Hoskins(1976), we take M to be the same three basic meridional profiles as theirs,

$$\begin{aligned}
M(\mu) &= \sin^2 \pi\mu, \quad \text{for } 30^\circ \text{ jet,} \\
&= \frac{\mu^2 \{6.75(1-\mu^2)\}^{1/2}}{1 + 9(\mu^2 - \frac{2}{3})^2}, \quad \text{for } 55^\circ \text{ jet,} \\
&= (1-\mu^2)^{1/2}, \quad \text{for solid body rotation.} \quad (5.55)
\end{aligned}$$

Fig. 5,1, taken from Simmons and Hoskins(1976), shows the meridional cross sections of these three basic zonal flows and temperatures. We note that their basic flows are not linear functions of height. Furthermore, their basic state temperature fields are functions of both latitude and height, therefore their static stability parameters are not constant. Since these basic state parameters are not identical to ours, we can not directly compare their solutions with our solutions. To derive an equivalent constant static stability, we take the horizontal averaged temperature(Hoskins and Simmons,1975; Simmons and Hoskins, 1975) to calculate N^2 , then take the vertical average of it. For U_0 , we take their value of the mean flow at the meridional maximum and at 350 mb, which is approximately $z=1$ in our model. The scale height is calculated from the hemispherical mean temperature. Therefore we find

$$N_0^2 \cong 2.0 \times 10^{-4} \text{ sec}^{-2}, \quad H \cong 7.4 \text{ km} \quad \text{and} \quad \varepsilon \cong 0.11$$

Since β_s is a function U_0 , its value for each profile is

$$\begin{aligned}
\beta_s &= 0.39, \quad \text{for } 30^\circ \text{ jet} \\
&= 0.53, \quad \text{for } 55^\circ \text{ jet} \\
&= 0.59, \quad \text{for solid body rotation.}
\end{aligned}$$

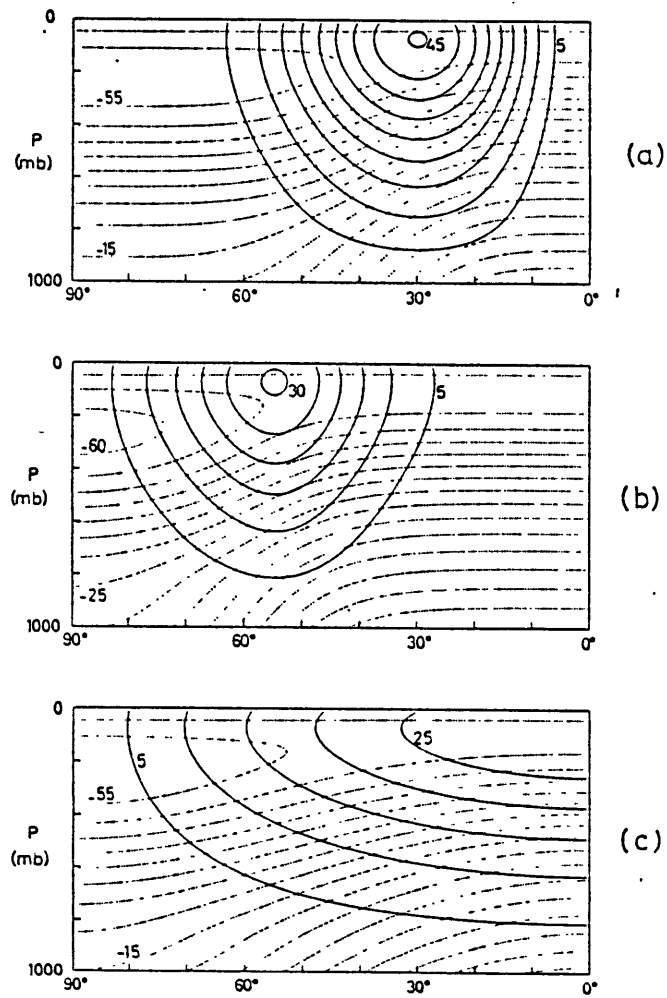


Fig. 5.1. The meridional cross sections of the basic flows and temperatures for the 30° jet (a), the 55° jet (b), and for solid body rotation (c), taken from Simmons and Hoskins(1976).

(a). The perturbation's growth rate and phase speed

To $O(\varepsilon)$, in dimensional form, the phase speed can be written as

$$c_r^* = \frac{M(\mu_0)U_0}{k} \frac{f_0}{N_0 H} \left\{ 1 + \frac{a(1-\mu_0^2)^{1/2}}{k} \frac{f_0}{N_0 H} \left[\frac{1}{2} - 0.67(1+\gamma) \right] \right\} \quad (5.56)$$

where γ is a general form of (4.87),

$$\gamma = \frac{\beta_0 N_0^2 H^2}{f_0^2 M(\mu_0) U_0} \quad (5.57)$$

f_0 and β_0 are the Coriolis parameter and its gradient at the turning point. To $O(\varepsilon^2)$, the dimensional growth rate is

$$\sigma_i = 0.425(1+\gamma) \frac{M(\mu_0)U_0}{k} \frac{f_0^2}{N_0^2 H^2} \left\{ 1 - \frac{a(1-\mu_0^2)^{1/2}}{k} \frac{f_0}{N_0 H} \left[0.26(1+\gamma) + \frac{0.67\gamma}{1+\gamma} \right] \right\} \quad (5.58)$$

We note that the growth rate and phase speed are determined at the turning point. Since the location of the turning point depends on M , c will be determined at different locations for different meridional profiles of the basic flow. As expected, if M is a solid body rotation, then (5.56) and (5.58) are identical to (4.84) and (4.88). Therefore these expressions are the general forms for the perturbation's growth rate and phase speed. Furthermore, since

$M(\mu_0)U_0$ is the characteristic velocity of the basic flow at the turning point, these expressions are similar to the perturbation's growth rate and phase speed for a uniform zonal flow on a β -plane. Hence, with a proper choice of the basic state parameters, a uniform zonal flow problem on a β -plane may be able to provide correct results about the perturbation's phase speed and growth rate. This may be the reason that, as indicated by Simmons and Hoskins(1976), there is much similarity between the β -plane and spherical calculations.

Figs. 5.2 to 5.7 show the growth rates and the phase speeds as functions of the zonal wavenumber k for the solid body rotation, the 30° jet and for the 55° jet. The "short wave" results were calculated from (5.56) and (5.58). The PE and QG results, taken from Simmons and Hoskins(1976), were calculated from the primitive equations and the quasigeostrophic equations, respectively. We note that the magnitudes of the growth rate and the phase speeds from these analytic expressions are generally in agreement with the numerical calculations. As expected, shorter waves give better agreement. Except for the solid body rotation case, the wavenumbers of the maximum growth rate and phase speed based on the approximate expressions do not agree with those of Simmons and Hoskins. Since the most unstable waves are near the limit of the shortwave approximation, the perturbation expansions of (5.56) and (5.58) can not provide accurate growth rates and phase speeds for these waves. Furthermore, the two-scale assumption has implicitly assumed that the meridional scale of the basic flow is larger than the perturbation's meridional scale, and thus the accuracy of (5.56) and

(5.58) may also be affected by the meridional scale of the basic flow. Since the meridional scales of the jet profiles are much narrower than the scale of the solid body rotation, the approximate expressions give poorer results for the jet profiles.

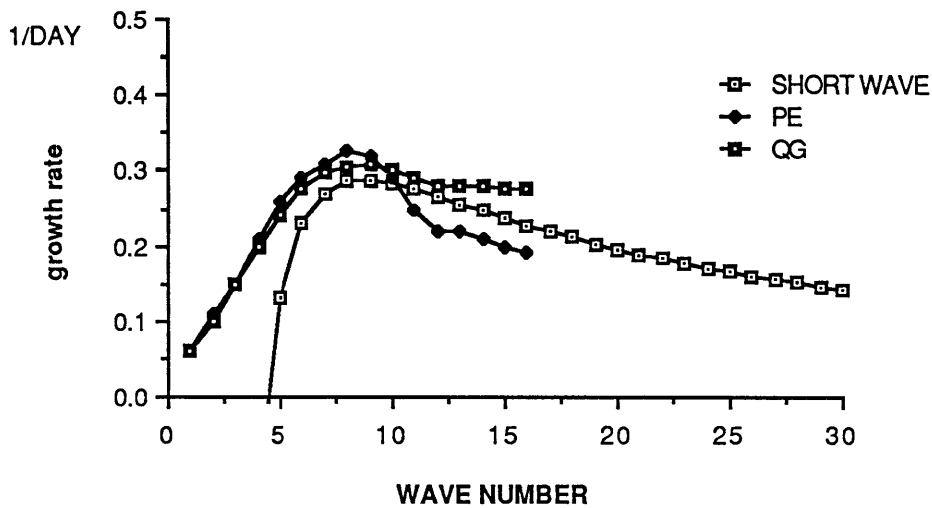


Fig. 5.2. The perturbation's growth rates as functions of the zonal wavenumber for the solid body rotation: the "Short wave" results were calculated from (5.58), PE and QG results, taken from Simmons and Hoskins(1976), were calculated from the primitive equations and the quasigeostrophic equations, respectively.

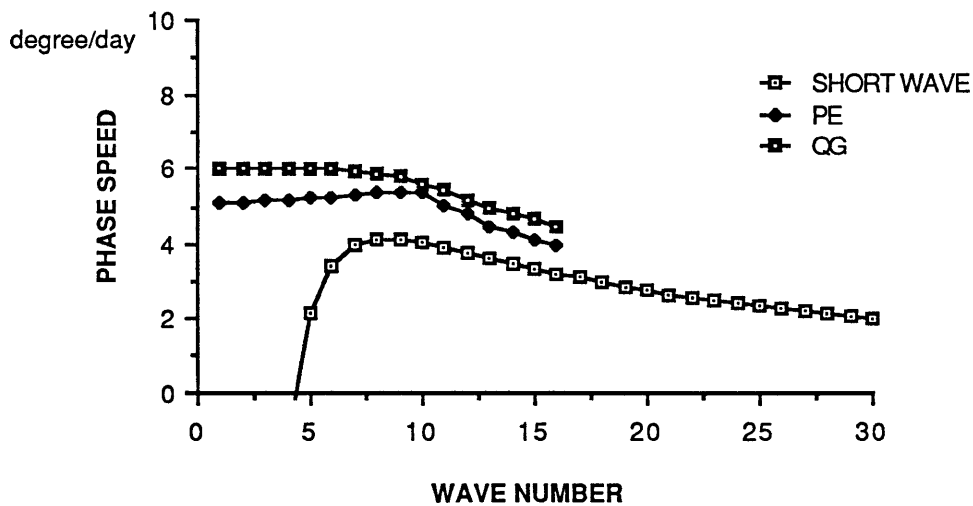


Fig. 5.3. As in fig. 5.2, except for the phase speeds.

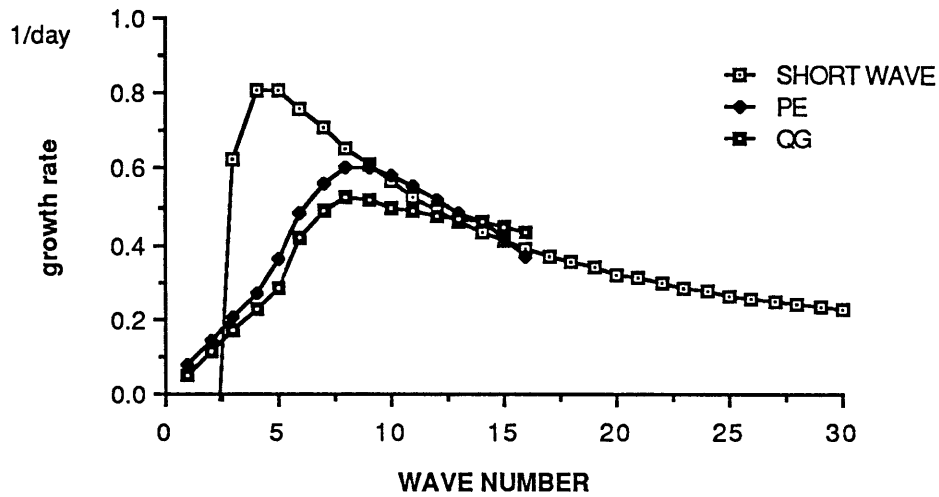


Fig. 5.4. The perturbation's growth rates as functions of the zonal wavenumber for the 30° jet.

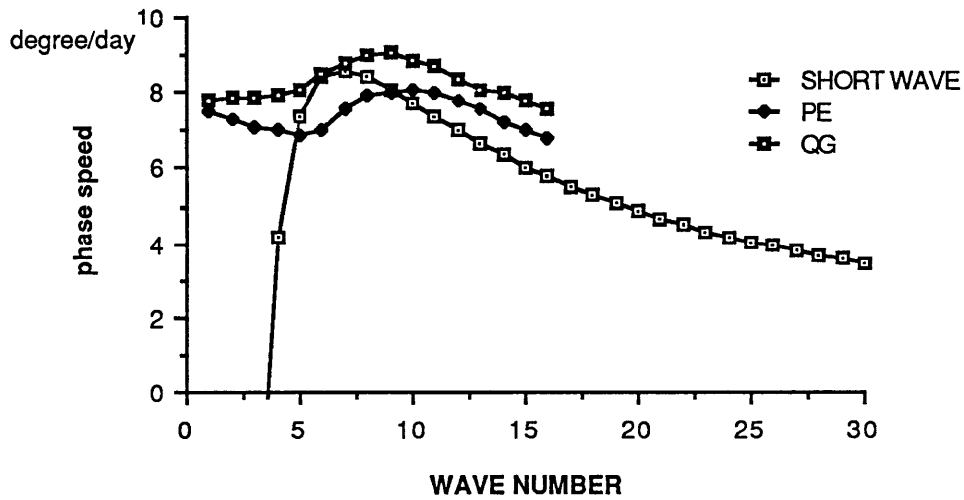


Fig. 5.5. As in fig. 5.4, except for the phase speeds.

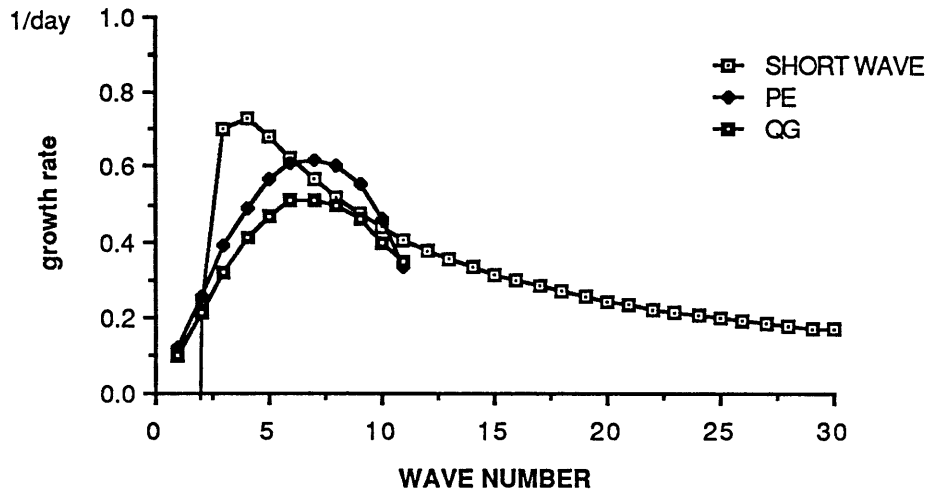


Fig. 5.6. The perturbation's growth rates as functions of the zonal wavenumber for the 55° jet.

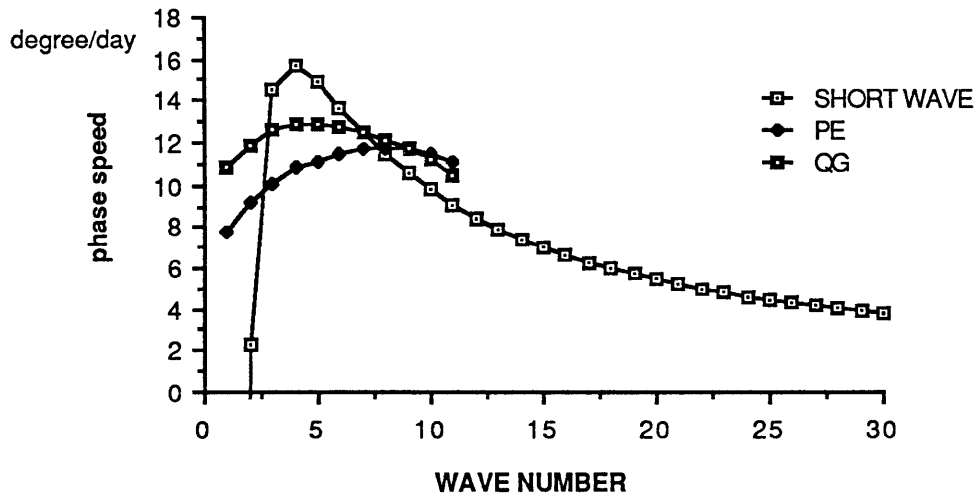


Fig. 5.7. As in fig. 5.4, except for the phase speeds.

(b). The meridional structures of the unstable waves

As discussed in chapter iv, the primary meridional structure is near the turning point. Since y and k were scaled by ε^{-1} and ε^{-2} , the meridional scale has a scale of $O(k^{1/2})$. From (5.50), for $n=1$, the perturbation's maximum amplitude is located at

$$\mu_m = \mu_0 + \frac{\varepsilon D_1}{2D_0} \quad (5.59)$$

We note that μ_0 is the leading order approximation of μ_m . Since D_0 and D_1 depend on k , μ_m depends weakly on the zonal wavenumber. Fig. 5.8 shows μ_m as a function of k for the solid body rotation, the 30° jet and for the 55° jet. The straight lines are the locations of the turning point for these three profiles. We note that the distance between μ_0 and the meridional maximum of the basic flow depends on the meridional scale of the basic flow. Furthermore μ_m converges to μ_0 more quickly for the jet profiles than for the solid body rotation.

The leading order phase of the meridional structure is

$$\alpha_\mu = -\operatorname{Im}\left\{ \varepsilon^{-2} \int_{\mu_0}^{\mu} (Q^2)^{1/2} d\mu \right\}, \quad \text{for } \mu > \mu_0 + O(\varepsilon)$$

$$\alpha_{\mu} = \varepsilon^{-1} \frac{D_{1i}}{2D_0^{1/2}} (\mu - \mu_0), \quad \text{for } \mu_0 - O(\varepsilon) < \mu < \mu_0 + O(\varepsilon)$$

$$\alpha_{\mu} = \text{Im} \left\{ \varepsilon^{-2} \int_{\mu_0}^{\mu} (Q^2)^{1/2} d\mu \right\}, \quad \text{for } \mu < \mu_0 - O(\varepsilon)$$
(5.60)

Figs. 5.9 to 5.11 show the amplitudes and phases for zonal wavenumber 8 as functions of latitude for those three profiles. As mentioned in the previous chapter, the amplitude decays rapidly away from the turning points. Since the solid body rotation has the largest meridional scale, its perturbation also has the largest meridional scale. Therefore the perturbation's meridional scale not only depends on the zonal wavenumber but also depends on the meridional scale of the basic flow. Although there are rapid variations of the phases near the equator or the pole, the amplitudes are small in these regions, and they do not have a significant effect on these unstable waves. Moreover we note that the gradients of the phases change sign for the jet profiles. Since the eddy momentum flux is proportional to the gradient of the phase, this implies that the eddy momentum fluxes will change sign for these two jet profiles.

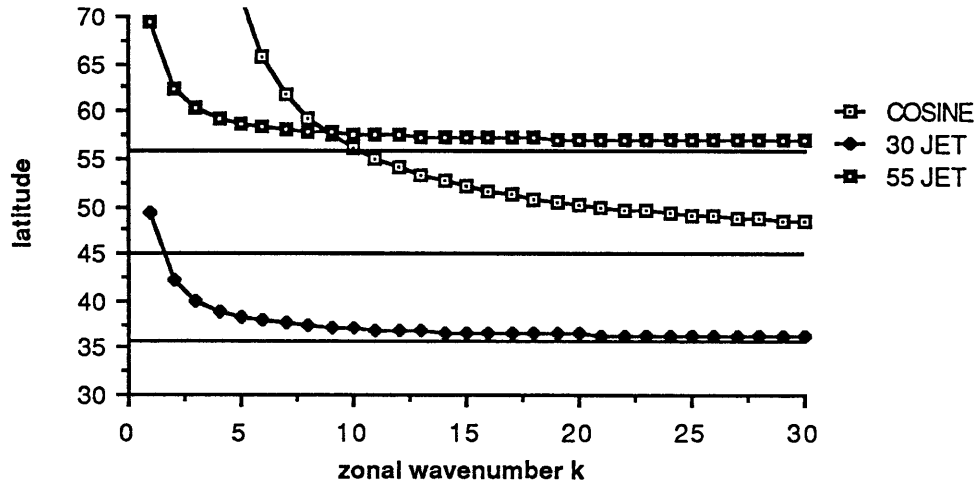


Fig. 5.8. The locations of the perturbation's maximum amplitude as functions of the zonal wavenumber for the solid body rotation, the 30° jet and for the 55° jet. The straight lines are the locations of the turning points for these three profiles.

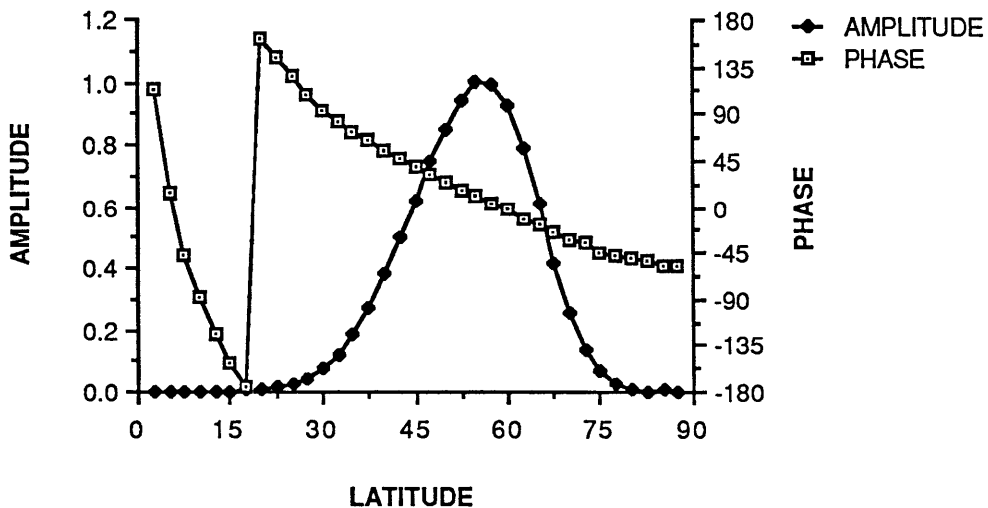


Fig. 5.9. The meridional amplitude and phase of the zonal wavenumber 8 as functions of latitude for the solid body rotation.

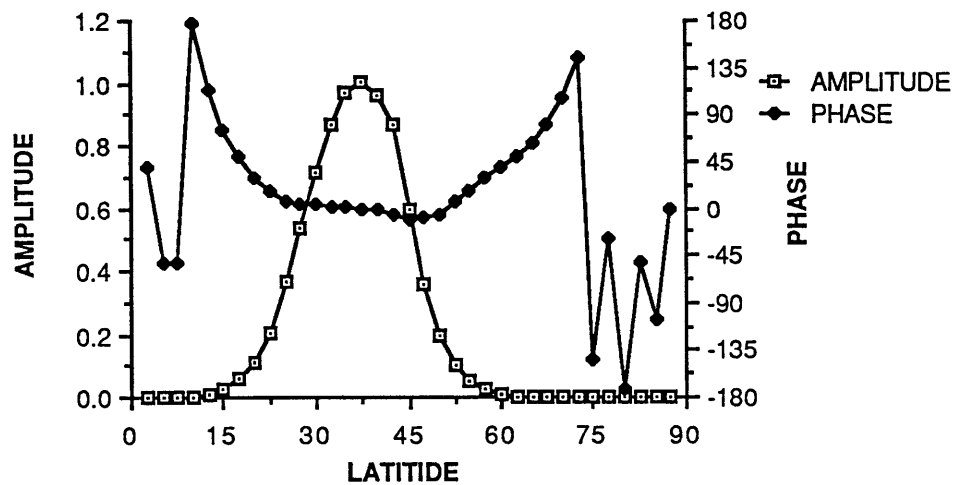


Fig. 5.10. As in fig.5.9, except for the 30⁰ jet.

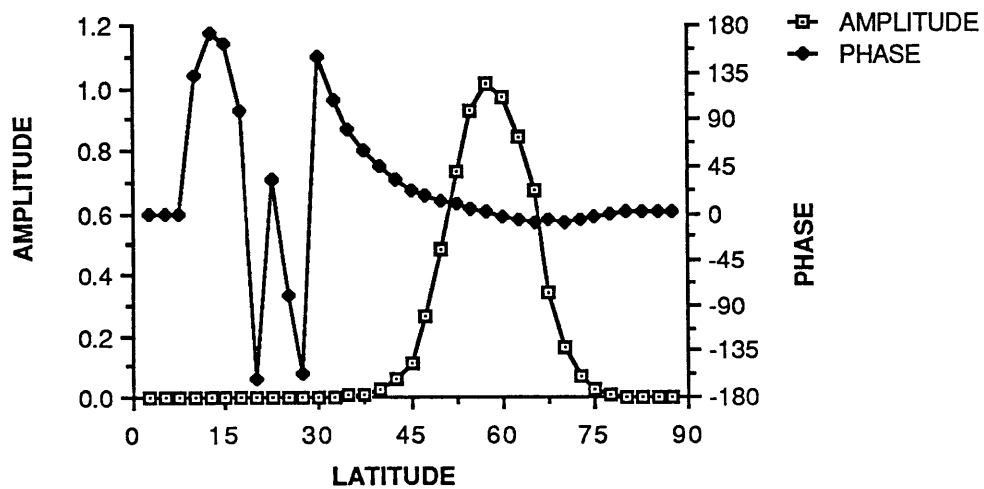


Fig. 5.11. As in fig.5.9, except for the 55⁰ jet.

(c). The vertical structures of the unstable waves

From (5.27), the perturbation's leading order vertical structure can be written as

$$\phi_0 = \exp\left\{ - \frac{M}{M(\mu_0)} \frac{k}{a(1-\mu^2)^{1/2}} \frac{N_0 H z}{f_0} + 1 \right\} \quad (5.61)$$

Thus ϕ_0 is an exponentially decreasing function of height. Since K_0 depends on k , as in chapter iv, the perturbation's vertical scale is proportional to the zonal scale. K_0 is also a function of M , except in the case of solid body rotation, so the perturbation's leading order vertical structure varies with latitude in general. The steering level is located at

$$z_s^* = c_r \frac{(1-\mu^2)^{1/2}}{M} H \quad (5.62)$$

Fig. 5.12 shows z_s^* at the turning point as a function of the zonal wavenumber for those three profiles. We note that the steering levels are near the lower boundary and decrease as waves become shorter. Since c_r is multiplied by $(1-\mu^2)^{1/2}/M$, although the perturbation's phase speeds showed significant differences among these three profiles, the steering levels at the turning points do not differ too much among these profiles.

Away from the critical layer, $\zeta=c_0(1-\mu^2)^{1/2}/M$, the leading order vertical phase α_v can be written as

$$\alpha_v = \tan^{-1} \left\{ \varepsilon e^{-2} \pi \zeta (b_0 - b) + \varepsilon \frac{b\pi}{2K_0} (e^{2(K_0\zeta-1)} - 1) H(K_0\zeta - 1) \right\} \quad (5.63)$$

where $H(x)=0$ if $x>0$ and $H(x)=1$ if $x<0$. Near $\zeta=c_0(1-\mu^2)^{1/2}/M$, α_v is

$$\alpha_v = \tan^{-1} \left\{ \frac{\varepsilon^{-1} e^{-2} \pi}{K_0} (b_0 - b) - \varepsilon b \left(\zeta - \frac{(1-\mu^2)^{1/2} c_r}{M} \right) \tan^{-1} \left(\frac{-\varepsilon \frac{c_i}{c_0}}{K_0 \zeta - \frac{c_r}{c_0}} \right) + \frac{\varepsilon \pi b}{K_0} (K_0 \zeta - 1) H(K_0 \zeta - 1) \right\} \quad (5.64)$$

Fig. 5.13 shows, to $O(\varepsilon)$, the amplitudes of the zonal wavenumber 8 at the turning point as functions of height for those three profiles. We note that, in general, the perturbation's amplitudes for these three basic flows are very similar. The amplitudes have maxima at the surface and decrease with height except near the critical layers. Fig. 5.14 shows the leading order vertical variation of the phases. The phase profiles also show similarities among the different basic flows. From these figures, we note that the meridional profile of the basic flow does not significantly affect the perturbation's vertical structure.

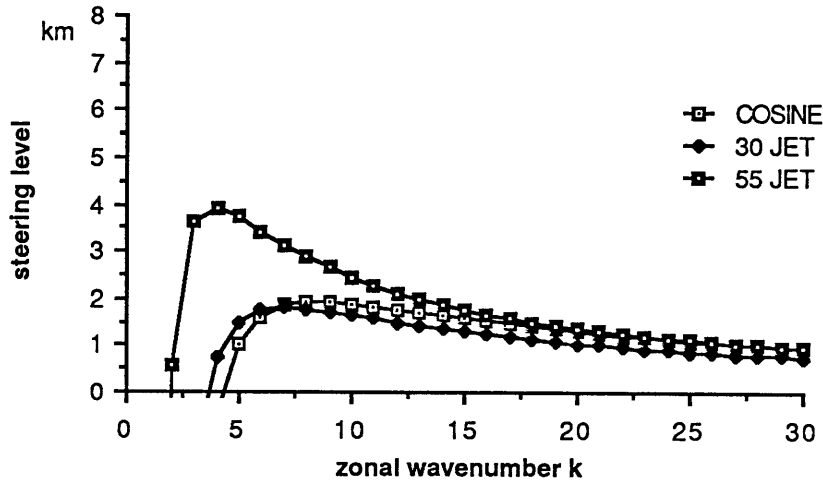


Fig. 5.12. The perturbation's steering levels at the turning point as functions of the zonal wavenumber for the solid body rotation, the 30° jet and for the 55° jet.

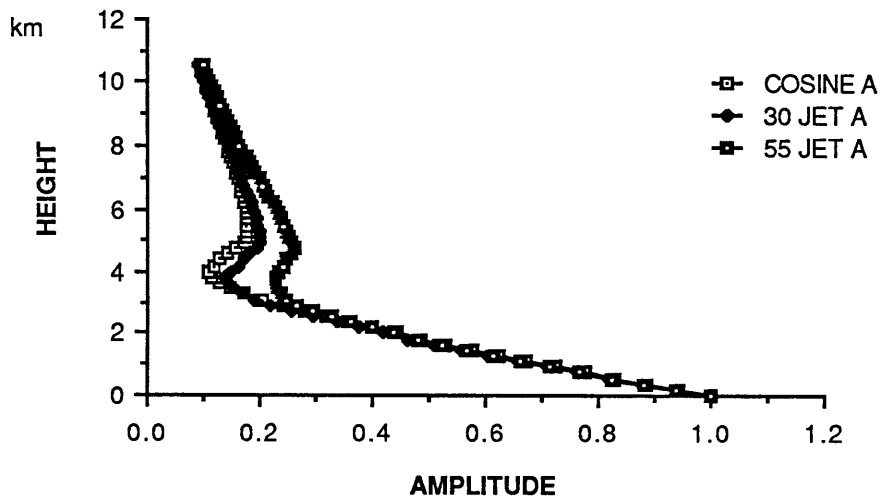


Fig. 5.13. The amplitudes of the zonal wavenumber 8 at the turning points as functions of height for the solid body rotation, the 30° jet and for the 55° jet.

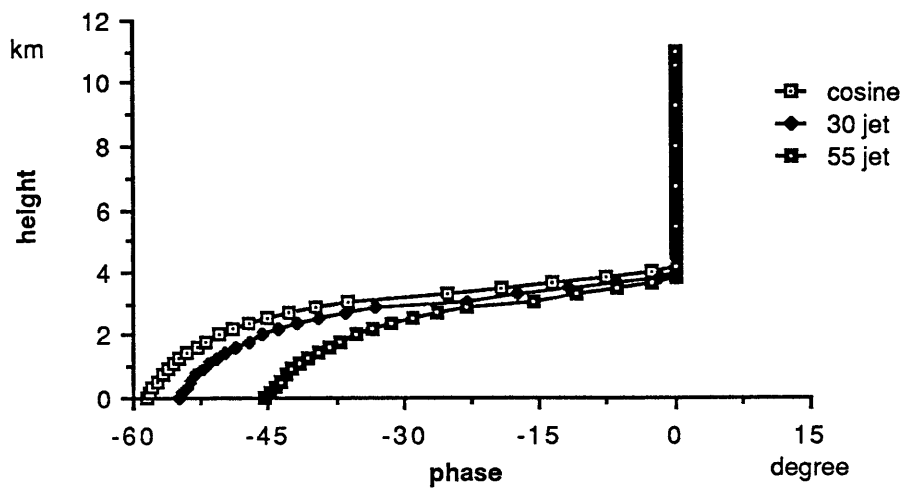


Fig 5.14. As in fig. 5.13, except for the leading order phase of the vertical structure.

(d). The eddy fluxes

The eddy heat and momentum fluxes are still given by (4.91) and (4.92). From (5.60), (5.63) and (5.64), we can derive the leading order of these eddy fluxes. Fig. 5.15 is the same as fig. 5.13, except for the vertical profiles of the leading order heat fluxes. Since the perturbation's vertical structure are similar for those three basic flows, the eddy heat fluxes are also very similar. These fluxes have maxima at the surface and decrease with height.

Fig. 5.16 shows the leading order eddy momentum flux as functions of latitude. Unlike the heat fluxes, these momentum fluxes differ significantly from profile to profile. As in chapter iv, the eddy momentum flux for the solid body rotation is poleward everywhere. The momentum flux for the 55° jet is mostly poleward, but there is very small equatorward flux at high latitudes. For the 30° jet, the momentum flux changes sign near the location of the perturbation's maximum amplitude. The equatorward flux is stronger than the poleward flux. Fig. 5.17, taken from Simmons and Hoskins(1976), shows the meridional cross sections of the momentum fluxes calculated from the primitive equations. The comparison between fig. 5.16 and 5.17 show that the momentum fluxes from the numerical calculations and from our approximate solutions are in good agreement. It seems that the analytic solutions of this study are able to capture the essential features of the momentum fluxes for different meridional profiles of the basic flows.

From (4.92), we note that the sign of the eddy momentum flux is determined by the perturbation's meridional phase gradient. From (5.60), the leading order meridional phase gradient can be written as

$$\begin{aligned}
 -\frac{\partial \alpha}{\partial \mu} &= -\varepsilon^{-1} \left(\frac{\mu^2}{1-\mu^2} \right)^{1/2} \frac{K_0}{D^{1/2}} K_{1i}, \quad \text{for } \mu > \mu_0 + O(\varepsilon) \\
 &= -\varepsilon^{-1} \frac{D_{1i}}{2D_0^{1/2}}, \quad \text{for } \mu_0 - O(\varepsilon) < \mu < \mu_0 + O(\varepsilon) \\
 &= \varepsilon^{-1} \left(\frac{\mu^2}{1-\mu^2} \right)^{1/2} \frac{K_0}{D^{1/2}} K_{1i}, \quad \text{for } \mu < \mu_0 - O(\varepsilon)
 \end{aligned} \tag{5.65}$$

where

$$D = \frac{k_0^2}{\mu^2(1-\mu^2)} - K_0^2 \tag{5.66}$$

Since D_{1i} is the μ derivative of K_{1i} at the turning point, the sign of (5.65) only depends on the function K_{1i} , which is

$$K_{1i} = e^{-2\pi} \left\{ \left(1 + \frac{\beta_s (1-\mu^2)^{1/2}}{\mu^2 M} \right) - \frac{M}{(1-\mu^2)^{1/2}} \frac{(1-\mu_0^2)^{1/2}}{M(\mu_0)} \left(1 + \frac{\beta_s (1-\mu_0^2)^{1/2}}{\mu_0^2 M(\mu_0)} \right) \right\} \tag{5.67}$$

We note that (5.67) only depends on M , μ_0 and β_s . Since μ_0 is determined by M only, for given M and β_s , we can determine K_{1i} as a function of latitude. It is easy to see that, without the β_s term, K_{1i} is zero for a solid body rotation. Therefore the existence of the β_s term is very important to correctly present the effect of the spherical

geometry on the baroclinic instability problem. From (5.65) and (5.67), we can see that the eddy momentum flux is positive at low latitudes for westerly flow. This is the same conclusion as that of Hollingsworth, Simmons and Hoskins(1976).

From (5.65), we note that, for the eddy momentum flux to change sign, K_{1i} must be zero somewhere other than the turning point. Therefore K_{1i} must have a minimum in the domain. Table 1. only shows the locations of the minima of K_{1i} for the observed seasonal averaged zonal flows(from Oort, 1983) and $\beta_s=0.5$. Different values of β_s do not cause much change of the locations. The existence of the minima in K_{1i} indicate that the eddy momentum fluxes will change sign for these observed flows. The locations of the minima K_{1i} vary with seasons and different zonal flows. This feature implies that the meridional profile of the basic flow has a very important role in determining the behavior of the eddy momentum flux. Moreover it implies that our solutions are sensitive to the meridional profile of the basic flow. Since the locations of $K_{1i}=0$ are close to each other and the minimum of K_{1i} is located in between for each observed zonal flow, the implies that the location of the minimum also close to the location of the maximum convergence of the eddy momentum flux. Table 2. shows the locations of zeros in the observed eddy momentum fluxes. We note that the zeros of the observed eddy momentum fluxes also vary with seasons, but the differences are not as great as in table 1. From table 1 and table 2, we note that our approximate solutions are able to predict the change of sign of the eddy momentum flux from the observed zonal

flow, but they are not able to predict accurately where the change of sign occurs or the location of the eddy momentum flux extremes.

Since the properties of the unstable waves are mainly determined at the turning point, which is located at the maximum of the meridional temperature gradient, the meridional variation of the basic flow is very important in determining the behavior of the unstable waves on the sphere. Although the analytic solutions are for a general meridional profile of the basic flow, because of the limitations of the perturbation expansion and the two-scale assumption, the meridional scale of the basic flow will affect the accuracy of these solutions. In particular the solutions break down if the basic flow is rapidly varying, otherwise they capture the essential properties of baroclinic instability on the sphere. Furthermore, our solutions show the very close relation between baroclinic instability on the sphere and that on a β -plane, if the β -plane is located at the proper latitude.

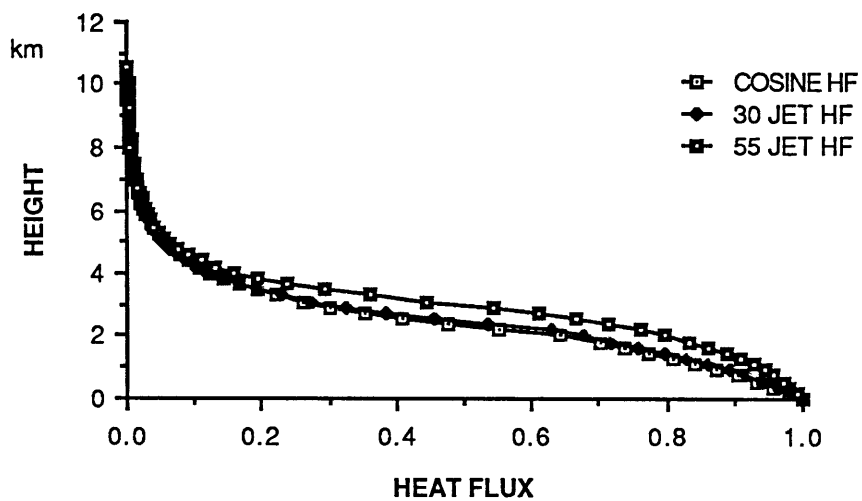


Fig. 5.15. As in fig. 5.13, except for the eddy heat fluxes.

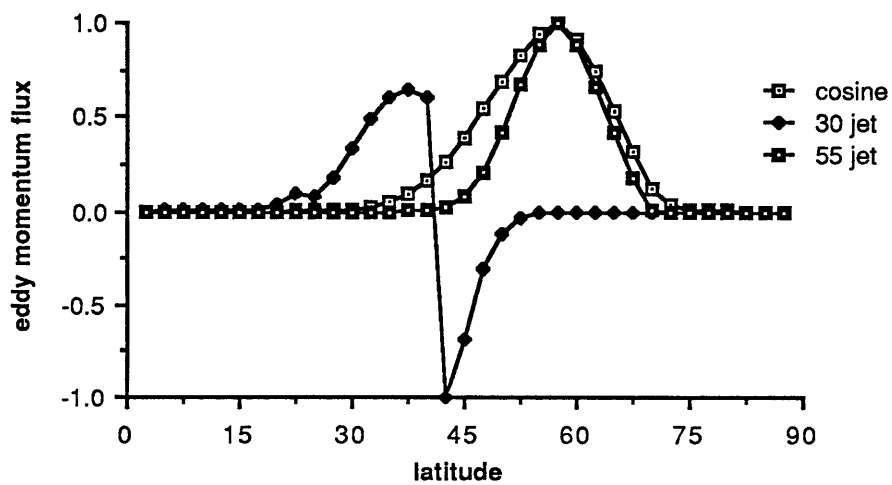


Fig. 5.16. The eddy momentum fluxes of zonal wavenumber 8 as functions of latitude for the solid body rotation, the 30° jet and for the 55° jet.

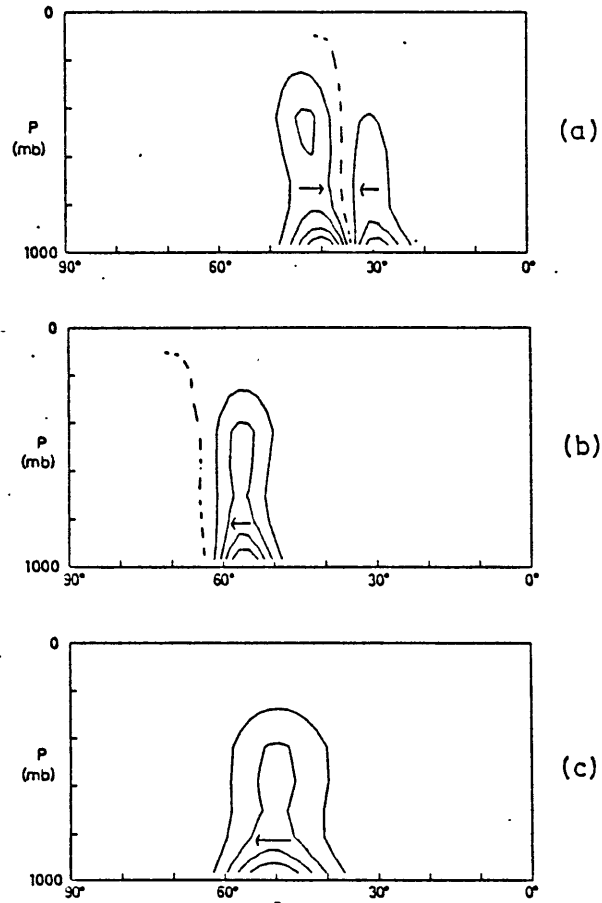


Fig. 5.17. The meridional cross sections of the eddy momentum fluxes at wavenumber 8 for the 30° jet (a), the 55° jet (b) and for solid body rotation (c), taken from Simmons and Hoskins(1976).

Table 1. The locations of the minima of K_{1i} for the observed zonal flows and $\beta_s = 0.5$, calculated from (5.67).

	Winter	Summer	Difference
U(200)	35^0	45^0	10^0
U(500)	40^0	50^0	10^0
U(850)	40^0	50^0	10^0
U(mean)	35^0	50^0	15^0
U(200)-U(850)	35^0	45^0	10^0

Table 2. The locations of zeros in observed eddy momentum fluxes. $[u'v']$ is the vertical averaged transient eddy momentum flux and $[u'v']+[u^*v^*]$ is the total flux, from Oort(1983)

	Winter	Summer	Difference
$[u'v']$	53^0	58^0	5^0
$[u'v']+[u^*v^*]$	51^0	57^0	6^0

CHAPTER VI

SUMMARY AND CONCLUSION

Since the quasigeostrophic potential vorticity equation on the sphere is analogous to the quasigeostrophic potential vorticity equation on a β -plane, we are able to apply some of the β -plane methods to perform an analytic study of the baroclinic instability problem on the sphere.

In chapter iii, we studied an analogue of Eady's problem on the sphere. The results are almost identical to those of Eady's model. Due to the absence of the basic state potential vorticity gradient, the spherical geometry does not play a significant role in determining the properties of the unstable waves and does not induce any eddy momentum flux.

In chapter iv, we developed a straightforward perturbation procedure to solve an analogue of Charney's problem on the sphere. This procedure, which consists of a shortwave approximation and a two-scale formalism, is able to obtain the analytic solutions for the baroclinic instability problem of a general meridional profile of the basic flow. Since we adopted the shortwave approximation, only a second-order turning point can exist in our perturbation solutions. The properties of the unstable waves on the sphere are mainly determined at this turning point. The perturbation's growth rate and phase speed are determined by the basic state parameters at the

turning point. The location of the perturbation's maximum amplitude strongly depends on the location of the turning point. Due to the presence of the β_s term in the equation, there is an eddy momentum flux in this problem. Since the β_s term is divided by μ^2 , the meridional variation of the Coriolis parameter has a significant effect on the properties of the unstable waves. As expected, the perturbation solutions are not valid at long waves. Moreover, the properties of the unstable waves and the valid range of the shortwave approximation are affected by the values of the basic state parameters.

In chapter v, we studied the baroclinic instability problem of a general meridional profile. From the perturbation solutions, we learned that the turning point is located at the maximum of the meridional temperature gradient, which is solely determined by the meridional profile of the basic flow. For a westerly mean flow, the turning point is always located on the poleward side of the mean flow maximum, which is the same conclusion as those of the numerical studies (Moura and Stone, 1976; Simmons and Hoskins, 1976). Furthermore, we found that the perturbation's growth rate, phase speed and the vertical structure at the turning point are very similar to those of Branscome (1983). Therefore, with a proper choice of the basic state parameters, the β -plane analysis of a uniform zonal flow can provide reasonable results for these properties of the unstable baroclinic waves on the sphere.

In comparison with the numerical study of Simmons and Hoskins(1976), the magnitudes of the perturbation's growth rate and phase speed from these perturbation solutions are in reasonable agreement with the numerical calculations. Except for the solid body rotation case, these perturbation solutions were unable to locate accurately the most unstable waves. This failure is caused by the limitations of both the shortwave approximation and the two-scale assumption. Since the turning point is determined by the meridional profile of the basic flow, the perturbation's meridional structures are different from profile to profile of the basic flow. But the perturbation's vertical structures at the turning points and the eddy heat fluxes did not show significant differences for different basic flows.

The comparison between the leading order eddy momentum fluxes and those of Simmons and Hoskins(1976) showed that they are in good agreement. From these analytic solutions, we noted that the sign of the eddy momentum flux only depends on the perturbation's meridional phase gradient. Since this gradient is mainly a function of the meridional profile of the basic flow, we can predict the sign of the eddy momentum flux from these perturbation solutions for a given meridional profile of the basic flow. In comparison with the observed eddy momentum flux, these analytic solutions were able to predict qualitatively correct latitudinal variations of the mean transient eddy momentum flux from the observed seasonal averaged zonal wind profile. However these analytic solutions are not able to determine accurately the locations

of the change of sign and of the eddy momentum flux extremes from the complex observed mean states, because of the linearization assumption (Edmon et al., 1980).

Although these analytic solutions have many limitations, i.e., the simplified basic states, the shortwave approximation and the two-scale assumption, they still capture the essential features of baroclinic instability on the sphere. From this study, we have learned

- (a). that there is a very close relationship between the baroclinic instability problem on the sphere and that on a β -plane,
- (b). how and where the properties of the baroclinic unstable waves are determined,
- (c). the effects of the spherical geometry and the meridional profile of the basic flow on the properties of the unstable waves.

These analytic solutions can be applied to predict the properties of the unstable waves for any given meridional profile of the basic flow. This information is of considerable value for guiding numerical studies and for improving parameterizations of eddy fluxes in climate modeling.

REFERENCES

- Abramowitz, M. and Stegun, I. A., 1964: *Handbook of Mathematical Functions*. National Bureau of Standards. Chapter 5.
- Bender, C. M. and S. A. Orszag, 1978: *Advanced Mathematical Methods for Scientists and Engineers*. McGraw-Hill, 593 pp.
- Branscome, L. E., 1983: The Charney stability problem: approximate solutions and modal structures. *J. Atmos. Sci.*, **40**, 1393-1409.
- Charney, J. G., 1947: The dynamics of long waves in a baroclinic westerly current. *J. Meteor.*, **4**, 135-162.
- Dickinson, R. E., 1968: On the exact and approximate linear theory of vertically propagating Rossby waves forced at a spherical lower boundary. *Mon. Weath. Rev.*, **96**, 405-414.
- Eady, E. T., 1949: Long waves and cyclone waves. *Tellus.*, **1**, 33-52.
- Edmon, H. J., B. J. Hoskins and M. E. McIntyre, 1980: Eliassen-Palm cross sections for the troposphere. *J. Atmos. Sci.*, **37**, 2600-2616.
- Frederiksen, J. S., 1978: Growth rates and phase speeds of baroclinic waves in multi-level models on a sphere. *J. Atmos. Sci.*, **35**, 1816-1826.
- Gent, P. R., 1974: Baroclinic instability of a slowly varying zonal flow. *J. Atmos. Sci.*, **31**, 1983-1994.
- Green, J. S. A., 1960: A problem in baroclinic instability. *Quart. J. Roy. Meteor. Soc.*, **86**, 237-251.

- Held, I. M., 1978: The vertical scale of an unstable baroclinic wave and its importance for eddy heat flux parameterization. *J. Atmos. Sci.*, **35**, 572-576.
- Hildebrand, F. B., 1963: *Advances Calculus for Applications*. Prentice-Hall, 646 pp.
- Hollingsworth, A., 1975: Baroclinic instability of a simple flow on the sphere. *Quart. J. Roy. Meteor. Soc.*, **101**, 495-528.
- _____, A. J. Simmons, B. J. Hoskins, 1976: The effect of spherical geometry on momentum transports in simple baroclinic flows. *Quart. J. Roy. Meteor. Soc.*, **102**, 901-911.
- Ioannou, B. A. and Lindzen R. S., 1986: Baroclinic instability in the presence of barotropic jets. *J. Atmos. Sci.*, **43**, 2999-3014.
- Killworth, P. D., 1980: Barotropic and baroclinic instability in rotating stratified fluids. *Dyn. Atmos. & Ocean.*, **4**, 143-184.
- Kuo, H.-L., 1952: Three-dimensional disturbances in a baroclinic zonal current. *J. Meteor.*, **9**, 260-278.
- _____, 1973: Dynamics of quasi-geostrophic flows and instability theory. *Advances in Applied Mechanics*, Vol. 13, Academic Press, 247-330.
- Lindzen, R. S. and A. S. Rosenthal, 1981: A WKB asymptotic analysis of baroclinic instability. *J. Atmos. Sci.*, **38**, 619-629.
- Lorenz, E. N., 1960: Energy and numerical weather prediction. *Tellus*, **12**, 448-464.

- McIntyre, M. E., 1970: On the nonseparable parallel flow instability problem. *J. Fluid. Mech.*, **40**, 273-306.
- Moura, A. D. and P. H. Stone, 1976: The effects of spherical geometry on baroclinic instability. *J. Atmos. Sci.*, **33**, 602-616.
- Oort, A. H., 1983: Global Atmospheric Circulation Statistics, 1958-1973. NOAA Professional Paper 14.
- Pedlosky, J., 1964a: The stability of currents in the atmosphere and the ocean. Part I. *J. Atmos. Sci.*, **21**, 201-219.
- _____, 1964b: The stability of currents in the atmosphere and the ocean. Part II. *J. Atmos. Sci.*, **21**, 342-353.
- _____, 1987: *Geophysical Fluid Dynamics*, Second edition. Springer-Verlag, 710 pp.
- Simmons, A. J., 1974: The meridional scale of baroclinic waves. *J. Atmos. Sci.*, **31**, 1515-1525.
- _____, and B. J. Hoskins, 1976: Baroclinic instability on the sphere: Normal modes of primitive and quasi-geostrophic equations. *J. Atmos. Sci.*, **33**, 1454-1477.
- Stone, P. H., 1969: The meridional structure of baroclinic waves. *J. Atmos. Sci.*, **26**, 376-389.

BIOGRAPHICAL NOTE

The author was born on February 15, 1957 in Taipei, Taiwan, Republic of China. He entered National Taiwan University in September, 1975 and graduated from there in June, 1979, receiving a B. S. degree in Atmospheric Sciences. He enter graduate school at M. I. T. in September, 1981.